

UNCLASSIFIED

AD 400 535

*Reproduced
by the*

**ARMED SERVICES TECHNICAL INFORMATION AGENCY
ARLINGTON HALL STATION
ARLINGTON 12, VIRGINIA**



UNCLASSIFIED

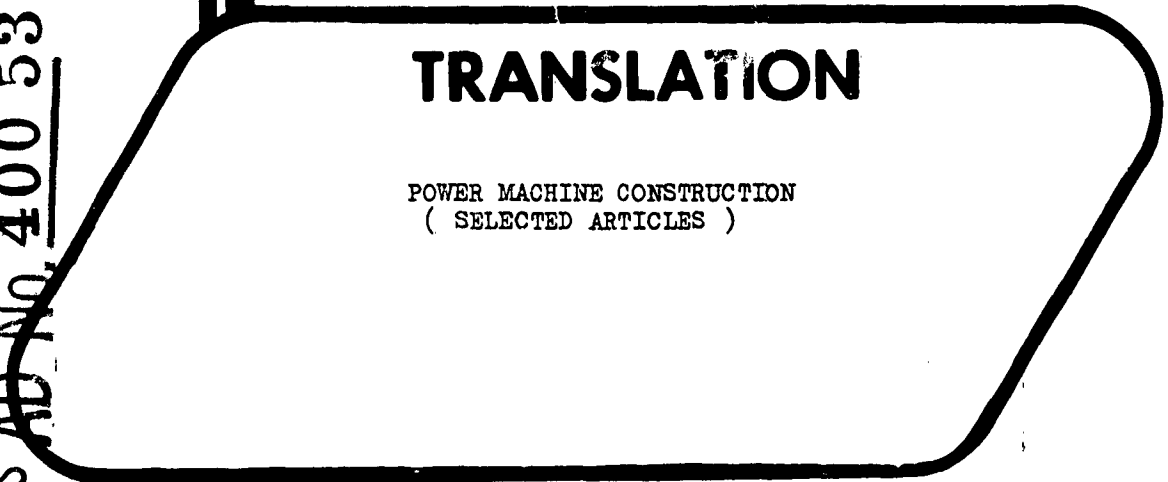
NOTICE: When government or other drawings, specifications or other data are used for any purpose other than in connection with a definitely related government procurement operation, the U. S. Government thereby incurs no responsibility, nor any obligation whatsoever; and the fact that the Government may have formulated, furnished, or in any way supplied the said drawings, specifications, or other data is not to be regarded by implication or otherwise as in any manner licensing the holder or any other person or corporation, or conveying any rights or permission to manufacture, use or sell any patented invention that may in any way be related thereto.

63-3-1

FTD-TT 62-1816

CATALOGED BY ASTIA
AS AD No. 400 535

400 535



TRANSLATION

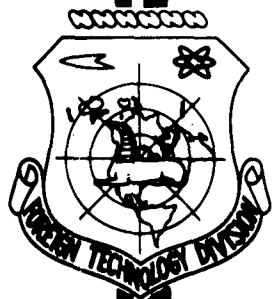
POWER MACHINE CONSTRUCTION
(SELECTED ARTICLES)

FOREIGN TECHNOLOGY DIVISION

AIR FORCE SYSTEMS COMMAND

WRIGHT-PATTERSON AIR FORCE BASE

OHIO



UNEDITED ROUGH DRAFT TRANSLATION

POWER MACHINE CONSTRUCTION (SELECTED ARTICLES)

English Pages: 80

Source: Russian Periodical, Energomashinostroyeniye,
No. 221, 1962, pp. 5-16, 17-31, 32-46, 103-109.

SC-1708-1711
SOV/563-62-0-221

THIS TRANSLATION IS A RENDITION OF THE ORIGINAL FOREIGN TEXT WITHOUT ANY ANALYTICAL OR EDITORIAL COMMENT. STATEMENTS OR THEORIES ADVOCATED OR IMPLIED ARE THOSE OF THE SOURCE AND DO NOT NECESSARILY REFLECT THE POSITION OR OPINION OF THE FOREIGN TECHNOLOGY DIVISION.

PREPARED BY:

TRANSLATION SERVICES BRANCH
FOREIGN TECHNOLOGY DIVISION
WF-AFB, OHIO.

TABEL OF CONTENTS

	Page
Study of the Operation of a Centrifugal Compressor Wheel, S. A. Anisimov.....	1
The Influence of the Number of Vanes on the Efficiency of the Centrifugal Wheel with a Single-Stage Cascade, S. A. Anisimov....	20
Study of the Efficiency of Centrifugal Compressor Wheels with a Two-Stage Vane Cascade, M. I. Kalinina.....	44
Calculation of Variable Regimes of Cascade Flow, V. A. Zysin.....	69

STUDY OF THE OPERATION OF A CENTRIFUGAL COMPRESSOR WHEEL*

S. A. Anisimov

The problem of creating highly efficient centrifugal compressors, at the modern level of the development of the theory of these machines, when theoretical methods alone do not assure sufficiently reliable results, can be successfully solved only by means of appropriate experimental work. Of great significance along these lines are experimental studies of centrifugal compressor wheels; when evaluating the efficiency of operation of the wheels it is necessary to take into account not only the basic characteristics of the wheel itself, but also the effect that the wheel has on the operation of the fixed elements, mainly on the diffuser. In other words, the operational efficiency of a wheel should be judged not only on the basis of its characteristics, but also on the basis of the structure of the flow behind the wheel.

The studies were made on the ETsK-1 stand at the Compressor Laboratory of the Kalinin Leningrad Polytechnic Institute [1]. In all, we studied 10 double-shrouded wheels with single-stage cascades;

* Docent K. P. Seleznev and Senior Engineer F. S. Rekstin participated in the work.

the only difference was in the number of blades. Figure 1 gives the basic geometric parameters of these wheels. In the article we give experimental data on a single wheel ($z = z_1 = z_2 = 16$),* since the principles established for the other wheels are principally of a similar nature.

Special observations were made for cases when the nature of the curves changed somewhat with a change in the number of blades z . The question of the influence of the number of blades on the efficiency of the wheels is treated separately in detail in the second article in this series (see p. 20).

A diagram of the blading of the ETsK-1 test stand and the control sections for measuring the individual flow parameters are given in Fig. 2 and have been treated in detail by Rekstin [1].

At cross section A-A (atmospheric conditions) we measured the temperature T_a with precision thermometers graduated to 0.1° C, and the barometric pressure P_a . At cross section 0-0, at the wheel eye, we measured the total pressure with a cylindrical ram-air pipe, and the static pressure through holes 0.7 mm in diameter in the housing of the inlet duct and the fairing. At cross section 3-3, behind the impeller, we determined the fields of temperature, angles, and total and static pressure using temperature probes and pneumometric heads. In addition we measured the static pressure through holes 0.7 mm in diameter in the forward wall of the diffuser and in the diaphragm.

The air output was determined using interchangeable metering nozzles, prepared and installed in the induction manifold according to the existing norms. The internal power was determined by two

* This wheel, with $z = 16$, was the best, from the standpoint of the realizable efficiency and head, of all the wheels investigated.

methods: by the drop in total pressure and by the reactive moment in the housing of the electric motor with a pivoting stator.

The number of revolutions of the shaft of the experimental stage was measured from the readings of an electrical tachometer and a total revolution counter.

The wheels were tested for a constant number of revolutions, $n = 14,900$ rpm ($u_2 = 214.5$ m/sec).

To evaluate the efficiency of the wheels we used the following criterional parameters: the adiabatic efficiency, by the total parameters η_{ad}^* and its relative value $\bar{\eta}_{ad}^*$; the head coefficients ψ^* , ψ , and φ ; the degrees of reaction Ω and ρ ; the coefficients of relative nonuniformity of flow k_α , k_G , $k_{h_{ad}}^*$ and k_{h_1} ; the absolute nonuniformity of flow $\Delta\alpha$; and the M and Re numbers. As the independent determining parameter we selected the flow factor φ_{ρ_0} (sometimes φ_ρ) and the angle of attack i_1 which is practically always associated with it.*

In our studies the Re number was arbitrarily determined, as is often done in the theory of centrifugal compressors, according to the formula

$$Re = \frac{u_2 D_2}{\nu_0} = \frac{\omega D_2^2 \gamma_0}{2\mu_0 g} \quad (1)$$

and was within the limits $(3.1-3.6) \times 10^6$.

The parameters were averaged in various ways. The average values of the parameters P_0 , P , and T_α were determined as the arithmetic means. The average values of the parameters ψ and h_{ad} were found

* The arbitrary designations used in the article, with few exceptions, are the same as the generally-accepted ones [2]. If not, explanations are given in the text.

The subscript of the parameters indicates the number of the control section to which the parameters pertain. The parameters behind the wheel, in cross section 3-3, are written without a subscript.

from previously averaged values of P_0 , P , and T_α . The average values of the parameters η_{ad}^* , ψ^* , φ , α , h_{ad}^* , h_l , and Ω were found by averaging their local values with respect to the flow. The average flow values G and φ_p were determined by measuring with a planimeter.

1. Results of the Investigation

1. Figure 3 shows the dependences $\eta_{ad}^* = f(\varphi_{p0})$ and $\bar{\eta}_{ad}^* = f(\varphi_{p0})$, where

$$\eta_{ad}^* = \frac{N_{ad}^*}{N_l} = \frac{G_0 h_{ad}^*}{G_0 h_l} = \frac{h_{ad}^*}{h_l}; \quad (2)$$

$$\bar{\eta}_{ad}^* = \frac{\eta_{ad}^*}{\eta_{ad}^* \max}; \quad (2')$$

$$h_{ad}^* = \frac{k}{k-1} RT_0^* \left[\left(\frac{p^*}{p_0} \right)^{\frac{k-1}{k}} - 1 \right]; \quad (3)$$

$$h_l = \frac{c_p}{A} (T^* - T_0^*); \quad (4)$$

$$\varphi_{p0} = \frac{c_{x0}}{\mu_0}. \quad (5)$$

For the value of φ_{p0} when $\eta_{ad}^* \max$ and ψ_{\max}^* we used, respectively, the designations $\varphi_{p0 \text{opt}}$ and $\varphi_{p0 \text{cr}}$.

The curve $\bar{\eta}_{ad}^* = f(\varphi_{p0})$ has an extreme value. The drop in efficiency to the left and to the right of the extreme value is explained by the large positive and negative angles of attack which cause a deterioration in the aerodynamics of the flow in the wheel, and by the appearance of developed separation zones.

The experimental data on $\bar{\eta}_{ad}^*$ obtained by various methods - according to temperatures ($\bar{\eta}_{ad}^* T$) and using a pendulum-motor ($\bar{\eta}_{ad}^* \text{pm}$) - are in good agreement. The maximum value of the efficiency attained for the given wheel $\eta_{ad}^* T \max = 0.9$.

The nature of the curve $\eta_{ad}^* = f(\varphi_{p0})$ depends on the number of blades. With a decrease in z the maximum efficiency is weakly

expressed, while when $z \leq 6$ it is generally not expressed at all.

2. The head coefficients shown in Fig. 3 were determined from the following formulas:

$$\psi^* = \frac{h_{ad}^*}{\frac{u_2^2}{2g}}; \quad (6)$$

$$\psi = \frac{h_{ad}}{\frac{u_2^2}{2g}}; \quad (7)$$

$$\varphi = \frac{c_u}{u_2}, \quad (8)$$

where

$$h_{ad} = \frac{k}{k-1} RT_0 \left[\left(\frac{p}{p_0} \right)^{\frac{k-1}{k}} - 1 \right]. \quad (9)$$

The curves of the head coefficients ψ^* , ψ , and φ have an extreme value.

In the optimum regime (at $\eta_{ad}^* \max$) these coefficients were $\psi^* = 1.28$, $\psi = 0.82$, and $\varphi = 0.695$. For the regime $i_1 = 0$ we obtained $\psi^* = 1.15$, $\psi = 0.75$, and $\varphi = 0.615$.

The decrease in the head coefficients ψ^* and φ with increased flow in the region $\varphi_{p_0} > \varphi_{p_0 cr}$ can be explained from an examination of the Stodola formula for the coefficient φ_2 (considering that the ratio $\varphi_{p_2}/\varphi_{p_0}$ is, for all intents and purposes, approximately constant):

$$\varphi_2 = \frac{c_{u_2}}{u_2} = 1 - \frac{\pi}{z_2} \sin \beta_{z_2} - \varphi_{p_2} \cot \beta_{z_2} = 1 - \frac{\pi}{z_2} \sin \beta_{z_2} - \frac{\varphi_{p_2}}{\varphi_{p_0}} \cot \beta_{z_2} \cdot \varphi_{p_0} \quad (10)$$

and on the basis of the connection between the coefficients φ and ψ^* :

$$\psi^* = 2\varphi(1 + \beta_{np} + \beta_{mp}) \eta_{ad}^*. \quad (11)$$

Formula (11) was obtained after transformations from Formulas (2) and (6), taking into account the relations

$$h_T = \varphi \frac{u_2^2}{g}; \quad (12)$$

$$h_i = h_T(1 + \beta_{np} + \beta_{mp}), \quad (13)$$

where, strictly speaking, by ψ^* and φ in Formula (11) we should understand ψ_2^* and φ_2 .

In addition, a drop in ψ^* and φ for large φ_{p_0} ($i_1 < 0$) is conditioned by a deterioration in the flow structure (the development of separation zones in the wheel channels).

The decrease in the head coefficients for low flow-rates ($\varphi_{p_0} < \varphi_{p_0cr}$) is explained by the sharp deterioration of the flow structure in the wheel with large positive angles of attack. In this region Formula (10) cannot be used.

The curves $\psi^* = f(\varphi_{p_0})$ and $\varphi = f(\varphi_{p_0})$ have approximately coincident maxima, while the curve $\psi^* = f(\varphi_{p_0})$ has great curvature. This can be explained by the structure of Formula (11), since the term $(1 + \beta_{np} + \beta_{mp})\eta_{a\partial}^*$ which characterizes the hydraulic energy losses is always less than unity, and in the investigated regime range is practically greater than 0.5.

The curvature of the curves $\varphi = f(\varphi_{p_0})$ and $\psi^* = f(\varphi_{p_0})$ depends on the number of blades. With decreasing z the curves become more sloping, so that at small z the maximum of the head coefficients is weakly expressed, while when $z \leq 6$ it is practically nonexistent.

3. The degrees of reaction Ω and ρ were determined from the following formulas:

$$\Omega = \frac{h_T - h_\partial}{h_T} = 1 - \frac{h_\partial}{h_T}; \quad (14)$$

$$\rho = \frac{h_{a\partial}}{h_{u\partial}} = \frac{h_{a\partial}^* - h_\partial}{h_{a\partial}^*} = 1 - \frac{h_\partial}{h_{a\partial}^*} = \frac{\psi}{\psi^*}; \quad (15)$$

where

$$h_\partial = \frac{c^2 - c_0^2}{2g} = (\varphi^2 + \varphi_p^2 - \varphi_{p_s}^2) \frac{u_2^2}{2g}. \quad (16)$$

Formulas (14) and (15), after appropriate transformations, can be reduced to the following approximate form which is convenient for analysis:

$$\Omega = 1 - \frac{\varphi^2 + \varphi_p^2 - \varphi_{p_0}^2}{2\varphi} \approx 1 - \frac{\varphi}{2}; \quad (14')$$

$$\rho = 1 - \frac{\varphi^2 + \varphi_p^2 - \varphi_{p_0}^2}{2\varphi(1 + \beta_{np} + \beta_{mp})\eta_{ad}^*} \approx 1 - \frac{\varphi}{2(1 + \beta_{np} + \beta_{mp})\eta_{ad}^*}, \quad (15')$$

since, for all practical purposes, $\varphi^2 \gg \varphi_p^2 - \varphi_{p_0}^2$, and therefore the difference $(\varphi_p^2 - \varphi_{p_0}^2)$ in these formulas can be disregarded.

The curves $\Omega = f(\varphi_{p_0})$ and $\rho = f(\varphi_{p_0})$ throughout the entire flow range, except for the region of large φ_{p_0} , are of identical nature. In this case, in the region of operating regimes (when $\varphi_{p_0} > \varphi_{p_0cr}$) with increasing φ_{p_0} the value of Ω continually increases, while the value of ρ first increases and then (at large φ_{p_0}) begins to decrease somewhat. This latter fact can be explained by the influence of energy losses. Quantitatively, Ω and ρ differ little from one another, except for the region of large φ_{p_0} .

The nature of the change in the degree of reaction with a change in flow rate can be explained using Formulas (14') and (15'). Since $(\varphi_p^2 - \varphi_{p_0}^2) \ll \varphi^2$, and it changes relatively insignificantly, we can conclude that the nature of the change in Ω will be approximately the reverse of the change in the value of φ . The value of ρ , as can be seen from Formula (15'), also depends on the energy losses; therefore its relation with φ will not be quite so simple. Since the value of $(1 + \beta_{np} + \beta_{mp})\eta_{ad}^*$ is always less than unity in all operating regimes, and since the adiabatic efficiency takes into account, in addition to leakage and web losses, losses in the blading of the wheel, it follows from Formulas (14') and (15') that $\Omega > \rho$. This is also confirmed by experimental data: in the optimum regime $\Omega = 0.68$ and $\rho = 0.64$, while in the regime $i_1 = 0$ we obtained $\Omega = 0.75$ and $\rho = 0.68$.

4. The curve $\varphi_p = c_r \sqrt{u_2} = f(\varphi_{p_0})$ has a dependence which is

close to linear, with a slight downward convexity (Fig. 3). In principle, this curve should pass through the coordinate origin. Quantitatively, φ_p and φ_{p_0} differ little from one another, but in this case for all operating regimes we have the inequality $\varphi_p < \varphi_{p_0}$. Their relation in the general case is defined as follows:

$$\frac{\varphi_p}{\varphi_{p_0}} = \frac{c_r}{c_{r_0}} = \frac{G}{G_0} \cdot \frac{F_0}{F} \cdot \frac{\gamma_0}{\gamma}$$

Analysis of the obtained experimental data shows that for the given wheel the ratio $\varphi_p/\varphi_{p_0} \approx \text{const.}$

5. The angle of attack when the flow enters the blades of the wheel is determined from the formula

$$i_1 = \beta_{g_1} - \beta_1 = \beta_{g_1} - \arctan \varphi_p \cdot \frac{F_0}{F_1} \cdot \frac{D_1}{D_2} \quad (17)$$

In this formula the inflow angle β_1 was determined without taking into account leakage through the packing on the covering disk and blockage of the channel; in addition, it was assumed that $\gamma_0 \approx \gamma_1$.

The curve $i_1 = f(\varphi_{p_0})$ has slight downward convexity. With increasing φ_{p_0} the algebraic value of i_1 continually decreases, which also follows from Formula (17).

The maximum efficiency was reached at $i_1 = +7^\circ$. The location of the optimum regime in the region of positive angles of attack can be explained, physically, by the fact that for normally backward bent vanes having negative angles of curvature of the radial cascade profile $\theta = \beta_{g_2} - \beta_{g_{2np}}$,* positive i_1 decrease the fluid deflection in

* $\beta_{g_{2np}}$ is the geometric angle at which the vanes come from the wheel, in which case for the given radial cascade we have rectilinear vanes. The values of this angle for vanes along the peripheral arc is determined from the formula $\cos \beta_{g_{2np}} = \cos \beta_{g_1} / (D_2/D_1)$. Since in centrifugal compressors $D_2/D_1 > 1$, then $\beta_{g_{2np}} > \beta_{g_1}$. If $D_2/D_1 = 1$, we have, approximately, $\beta_{g_{2np}} = \beta_{g_1}$ in the axial cascade, and consequently the angle $\theta = \beta_{g_1} - \beta_{g_1}$.

the radial cascade $\varepsilon = \beta_2 - \beta_{g_2 np} + 1^*$. (where $\beta_2 = \arctan \varphi_{2p}/1 - \varphi_2$), which evidently has a favorable effect on the aerodynamics of the flow in the wheel channels. For the given wheel $\beta_{g_2 np} = 63^\circ 57'$ and, consequently, $\theta = 49^\circ - 63^\circ 57' = -14^\circ 57'$.

The regime $\eta_{ad}^* \max$ has the corresponding angle $\beta_2 = 37^\circ 30'$ and, consequently, $\varepsilon = 37^\circ 30' - 63^\circ 57' + 7^\circ \approx -19^\circ 27'$. Figure 3 shows the dependences $\varepsilon = f(\varphi_{p_0})$ and $\beta_2 = f(\varphi_{p_0})$. Experimental data show that for the investigated series of wheels the nature and position of the curves $\varepsilon = f(\varphi_{p_0})$ and $\beta_2 = f(\varphi_{p_0})$ are practically independent of the number of vanes. For all the investigated wheels there is a sharp increase in the angle β_2 for low flow-rates, right up to $\varphi_{p_0} \approx 0.3$ ** while the minimum values of the absolute magnitudes of the angles ε are in the region $\varphi_{p_0} = 0.18-0.23$, close to $\varphi_{p_0 opt}$. We should mention that for the examined wheel with $z = 16$ which, as we have already stated, was optimum from the standpoint of efficiency, the minimum value of the absolute magnitude of ε ($|\varepsilon_{min}| \approx 17^\circ$) was the smallest of all the investigated wheels.

6. The general expression for determining the coefficients of the relative nonuniformity of flow according to the angle k_α , the flow rate k_G , and the absolute and internal heads $k_{h_{ad}}^*$ and k_{h_1} , shown in Fig. 3, had the form

$$k_\Pi = \frac{\Pi_{max} - \Pi_{min}}{\Pi} \quad (18)$$

where Π is a measureable parameter, averaged over the width of the channel; and Π_{max} and Π_{min} are the maximum and minimum values of the

* For an axial cascade (i.e., when $\beta_{g_2 np} = \beta_{g_1}$) $\beta_{g_1} = \beta_1 + 1$, and $\varepsilon = \beta_2 - \beta_1$.

** For other z 's in the region $\varphi_{p_0} > 0.3$ the intensity of the increase in β_2 also decreases, but not quite so strongly as was the case with the given wheel.

parameter Π over the width of the channel.

The larger the coefficient k_{Π} , the greater the relative nonuniformity.

The relative nonuniformity of flow with respect to energy, characterized by the coefficients $k_{h_{a\delta}^*}$ and k_{h_1} respectively as a function of the regime, changed but little. The absolute values of the relative nonuniformity of the flow with respect to energy are very small (the coefficients $k_{h_{a\delta}^*}$ and k_{h_1} are close to zero). A certain increase in $k_{h_{a\delta}^*}$ and k_{h_1} is observed for negative i_1 (large φ_{p_0}), and a very insignificant one is observed in the region of positive i_1 (small φ_{p_0}). Such an increase in the coefficients of relative nonuniformity is evidently a result of the deterioration of the flow structure of the impeller for rather large positive and negative angles of attack.

The relative nonuniformity of flow with respect to flow-rate and angle, characterized by the coefficients k_G and k_α , for angles of attack $i_1 \approx 0$ and regimes close to optimum, i.e., when $\eta_{a\delta}^* \max$ is slight compared with other regimes ($k_G \approx k_\alpha \approx 0.25-0.4$). For large positive angles of attack the coefficients of nonuniformity k_G and k_α greatly increase, reaching a comparatively high value ($k_G \approx k_\alpha \approx 4-4.5$). The sharp increase in the coefficients k_G and k_α for low flow-rates is explained not only by the deterioration in the flow structure, but also by the decrease in the absolute average values of G and α . For negative angles of attack with increasing φ_{p_0} the relative nonuniformity with respect to angle and flow rate increase insignificantly.

When analyzing the operation of the stage with the vaned diffuser, a great role is played by the numerical values of the deviations of the angle from the average angle. Figure 3 shows the dependences of

$\alpha = f(\varphi_{p0})$ and the absolute nonuniformity with respect to the angle $\Delta\alpha = \alpha_{\max} - \alpha_{\min} = f(\varphi_{p0})$. The graphs show that α , with a change in flow rate, changes within broad limits and continually increases with increasing φ_{p0} . The curve $\Delta\alpha = f(\varphi_{p0})$ has a minimum for regimes corresponding approximately to $\eta_{ad}^* \max$ and $i_1 \approx 0$. The increase in $\Delta\alpha$ in the region of large positive and negative angles of attack is explained by the deterioration of the flow structure within the impeller due to nonoptimal flow past the vaned apparatus and the influence of bending of the flow at the wheel inlet.

In the region of the investigated regimes, the maximum value of the absolute nonuniformity of flow with respect to the angle $\Delta\alpha$ reached 20° , while for the regimes $\eta_{ad}^* \max$ and $i_1 = 0$ it was within limits of 70° .

7. The curves $\varphi_p = f(X)$ (Fig. 4) show that for average φ_{p0} , the maximum flow rate (maximum φ_p) occurs near the forward wall of the vaneless diffuser, while for large φ_{p0} it occurs at the rear wall. Thus, with increasing gas flow through the wheel there is a displacement of the flow maximum from the forward to the rear wall. In addition, the nature of the curves $\varphi_p = f(X)$ attests to the fact that near the forward wall of the diffuser the gas flow across the section, for the majority of regimes, changes more sharply than at the rear wall. For low flow rates, reciprocal flows are noted at the walls.

The redistribution of the flow in the meridional cross section of the channel with increasing φ_{p0} can evidently be explained by the gradual development of separation behind the bend at the inlet to the inner surface of the covering disk due to increased diffusivity in

this zone with increasing $c_{z_0}^*$.

8. The nature of the curves $\alpha = f(X)$ shown in Fig. 4 is basically the same as that of the curves $\varphi_p = f(X)$.

9. The curve $\varphi = f(X)$, for average and high flow rates, qualitatively has a shape which is approximately the opposite of that of the curve $\varphi_p = f(X)$, which also follows from Formula (10). For low flow rates, however, this connection is not noted, which attests to the inapplicability of the Stodola formula when $\varphi_{p_0} < \varphi_{p_0 cr}$.

10. The curves $\psi^* = f(X)$ have basically the same nature as the curves $\varphi = f(X)$.

11. The drop in temperature ΔT^* characterizes, for all practical purposes, the head h_1 and, consequently, to a certain extent (without taking into account disk and slit energy losses) the coefficient φ .

The nature of the change in the curves $\Delta T^* = f(X)$ and $\varphi = f(X)$ should therefore be approximately analogous, which is verified by the derived experimental curves. Maximum deviation between the nature of these curves is noted for low flow rates due to the relative increase in the leakage of gas at the covering disk and disk losses, which also follows from the theoretical relation

$$\Delta T^* \dots \frac{A h_i}{c_p} = \frac{A}{c_p} \varphi \frac{u_2^2}{g} (1 + \beta_{np} + \beta_{mp}) = c \varphi (1 + \beta_{np} + \beta_{mp}), \quad (19)$$

where $c = (A/c_p)(u_2^2/g) = \text{const.}$

12. The nature of the change in the numbers M_{w_1} , M_{w_1}'' and M_c , and also M_{c_0} , as a function of the wheel regime is shown in Fig. 5.

These M numbers were determined as follows (Fig. 6):

* It is evident that the flow structure behind the wheel will also be a function of the shape of the meridional cross section of the wheel. We can also assume that the nature of the change in the curves $\varphi_p = f(X)$, $\alpha = f(X)$, $\varphi = f(X)$, $\psi^* = f(X)$ and $\Delta T^* = f(X)$ can be influenced by the leakage near the covering disk and through the diaphragm packing; however, this question requires special study.

$$M_{c_0} = \frac{c_0}{\sqrt{kgRT_0}}; \quad (20)$$

$$M_{w_1} = \frac{w_1}{\sqrt{kgRT_1}} \approx \frac{\sqrt{c_{r_1}^2 + u_1^2}}{\sqrt{kgRT_0}}; \quad (21)$$

$$M_{w_1}'' = \frac{w_1''}{\sqrt{kgRT_1}} \approx \frac{w_1'}{\sqrt{kgRT_0}} = M_{c_0} \frac{F_0}{F_1} \frac{1}{\tau_1 \sin \beta_{g_1}}; \quad (22)$$

where

$$w_1' = w_1 \frac{\sin \beta_1}{\tau_1 \sin \beta_{g_1}} = \sqrt{c_{r_1}^2 + u_1^2} \frac{\sin \beta_1}{\tau_1 \sin \beta_{g_1}} = \frac{c_{r_1}}{\tau_1 \sin \beta_{g_1}}; \quad (23)$$

$$M_c = \frac{c}{\sqrt{kgRT}}. \quad (24)$$

With increased gas flow, i.e., φ_{P_0} , the numbers M_{c_0} , M_{w_1} and particularly M_{w_1}'' increase. This also follows from an analysis of Formulas (20)-(23).

The number M_c depends little on the flow rate. In an optimal regime $M_{c_0} = 0.17$, $M_{w_1} = 0.37$, $M_c = 0.435$, $M_{w_1}'' = 0.51$. In the regime $i_1 = 0$, $M_{c_0} = 0.22$, $M_{w_1} = 0.4$, $M_c = 0.415$ and $M_{w_1}'' = 0.66$.

At the inlet to the impeller cascade with low flow rates ($i_1 > 0$) there is diffusivity (Fig. 6), i.e., $M_{w_1}''/M_{w_1} < 1$. With increasing flow rate the diffusivity decreases to zero and then, especially at $i_1 < 0$, effusivity rapidly increases, i.e., $M_{w_1}''/M_{w_1} > 1$.

The influence of the flow rate and the geometric parameters of the wheel on the velocity w_1'' and the number M_{w_1}'' is evident from Formulas (23) and (22). The ratio $\sin \beta_1 / \tau_1 \sin \beta_{g_1}$ defined by the angle of attack i_1 , since $i_1 = f(\beta_1, \beta_{g_1})$, and by the restriction of the

* The superscript (') for the parameter indicates that the given parameter is selected taking into account restriction of the flow by the vanes, while the superscript (") indicates, in addition, that account is taken of the bending of the flow at the inlet to an angle β_{g_1} . The value w_1'' is calculated somewhat more simply, without

taking into account the change in the geometric parameters from cross section B-B to section A-A (see Fig. 6). In the formulas it has been assumed that $T_0 \approx T_1 \approx T_1''$ and $c_{r_1} = c_1$.

flow at the inlet τ_1 , characterizes the diffusivity ($\sin \beta_1 / \tau_1 \sin \beta_{g_1} < 1$) or effusivity ($\sin \beta_1 / \tau_1 \sin \beta_{g_1} > 1$) on entry into the inter-vane channels of the wheel. With increasing gas flow rate and, consequently, increasing velocities c_{z_0} and c_{r_1} , the numbers M_{c_0} , M_{w_1} , M''_{w_1} will increase, as can be seen from Formulas (20), (21), and (22). But the intensity of the increase in M''_{w_1} , compared with M_{w_1} , in this case will be greater, since the ratio $\sin \beta_1 / \sin \beta_{g_1}$ will also increase due to an increase in the angle β_1 . Therefore with increasing flow rate the diffusivity at the inlet to the inter-vane channels should decrease. Theoretically, it follows from Formulas (21), (22), and (23) that with abnormally high restriction (very low τ_1), when the ratio $\sin \beta_1 / \tau_1 \sin \beta_{g_1} > 1$ and, consequently, $m''_{w_1} > M_{w_1}$, the diffuser zone will generally be absent at the inlet, even with large positive angles of attack.

The point of transition from a diffuser zone to an effuser one is determined by the condition

$$\frac{\sin \beta_1}{\tau_1 \sin \beta_{g_1}} = 1 \quad (25)$$

or, after transformation,

$$\varphi_{p_0 M} = \frac{\tau_1 \sin \beta_{g_1}}{\sqrt{1 - \tau_1^2 \sin^2 \beta_{g_1}}} \cdot \frac{F_1 \gamma_1}{F_0 \gamma_0} \cdot \frac{D_1}{D_0} \quad (26)$$

where $\varphi_{p_0 M}$ is the value of the flow factor φ_{p_0} for which $w_1 = w''_1$.

The point of intersection of the curves M_{w_1} and M''_{w_1} (Fig. 5), strictly speaking, is determined by the condition $M_{w_1} = M''_{w_1}$ or

$$\frac{\sin \beta_1}{\tau_1 \sin \beta_{g_1}} \sqrt{\frac{T_1}{T''_1}} = 1 \quad (27)$$

The ratio $\sqrt{T_1 / T''_1}$ when $M_{w_1} = M''_{w_1}$ is approximately equal to unity, which was assumed to be the case during the calculations. Therefore the point of intersection of the curves M_{w_1} and M''_{w_1} is treated as the

point of transition from a diffuser zone to an effuser one. This transition point is always in the region $i_1 > 0$, since $\tau_1 < 1$, and, consequently, $w_1 = w_1''$ only when $\sin \beta_1 / \sin \beta_{g_1} < 1$, i.e., $\beta_1 < \beta_{g_1}$ and $i_1 > 0$. The transition point can be found when $i_1 = 0$ only theoretically — in the absence of restriction, when $\tau_1 = 1$.

Conclusions

1. Investigation has made it possible to obtain a more complete understanding of the efficiency of operation of the wheel of a centrifugal compressor and to quantitatively associate individual experimental data with the results of theoretical analysis.

2. The attained efficiency $\eta_{ad}^* = 0.9$ is maximum for wheels with geometric parameters similar to the investigated wheels. For other geometric parameters, in particular the angles β_{g_2} and β_{g_1} , other peripheral velocities u_2 , etc., the efficiency level may change. For example, the transition to a two-stage cascade, as experimental data have shown (see p. 44), makes it possible to raise the efficiency of the wheel. A similar statement relative to the dependence of the obtained experimental data (mainly quantitative) on the initial geometry of the investigated wheels may be made for the other criterional parameters.

3. The experiments were conducted using wheels made according to the generally-accepted recommendations for typical wheels of stationary centrifugal compressors of limited performance. Therefore the obtained data on the values of the various criterional parameters of the wheel can be used directly mainly in designing the indicated compressors.

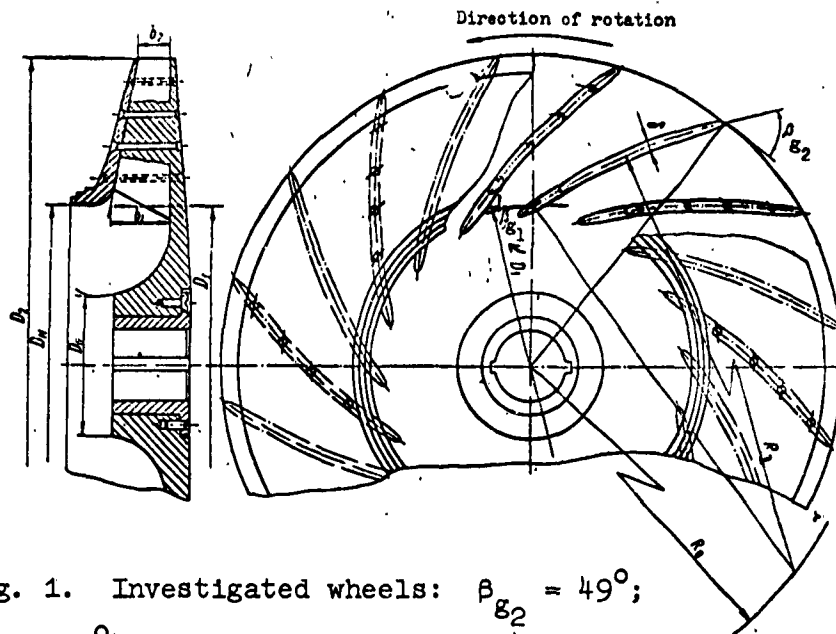


Fig. 1. Investigated wheels: $\beta_{g_2} = 49^\circ$;
 $\beta_{g_1} = 33^\circ 42'$; $D_2 = 275$ mm; $D_1 = 145$ mm;
 $D_{out} = 144$ mm; $D_0 = 65$ mm; $b_2 = 15$ mm; $b_1 =$
 $= 28$ mm; $\delta = 5$ mm; $R_0 = 171$ mm; $R_1 = 226.5$ mm;
 $z = z_1 = z_2 = 4-28$.

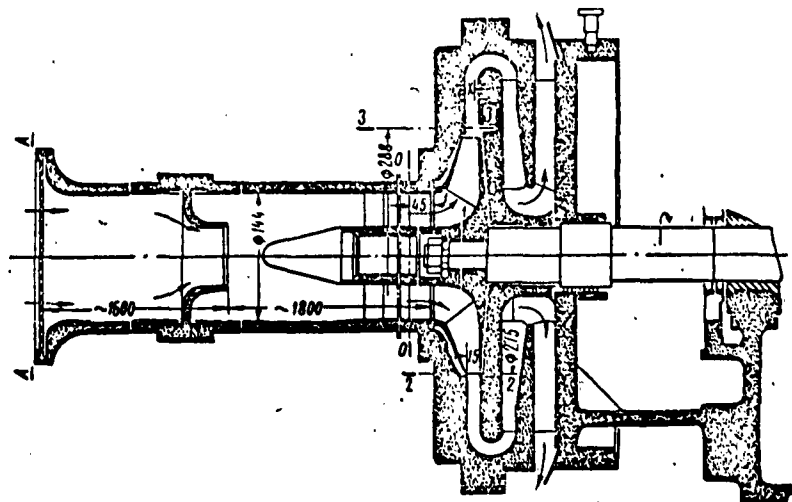


Fig. 2. Diagram of the blading
of the ETSK-1 stand.

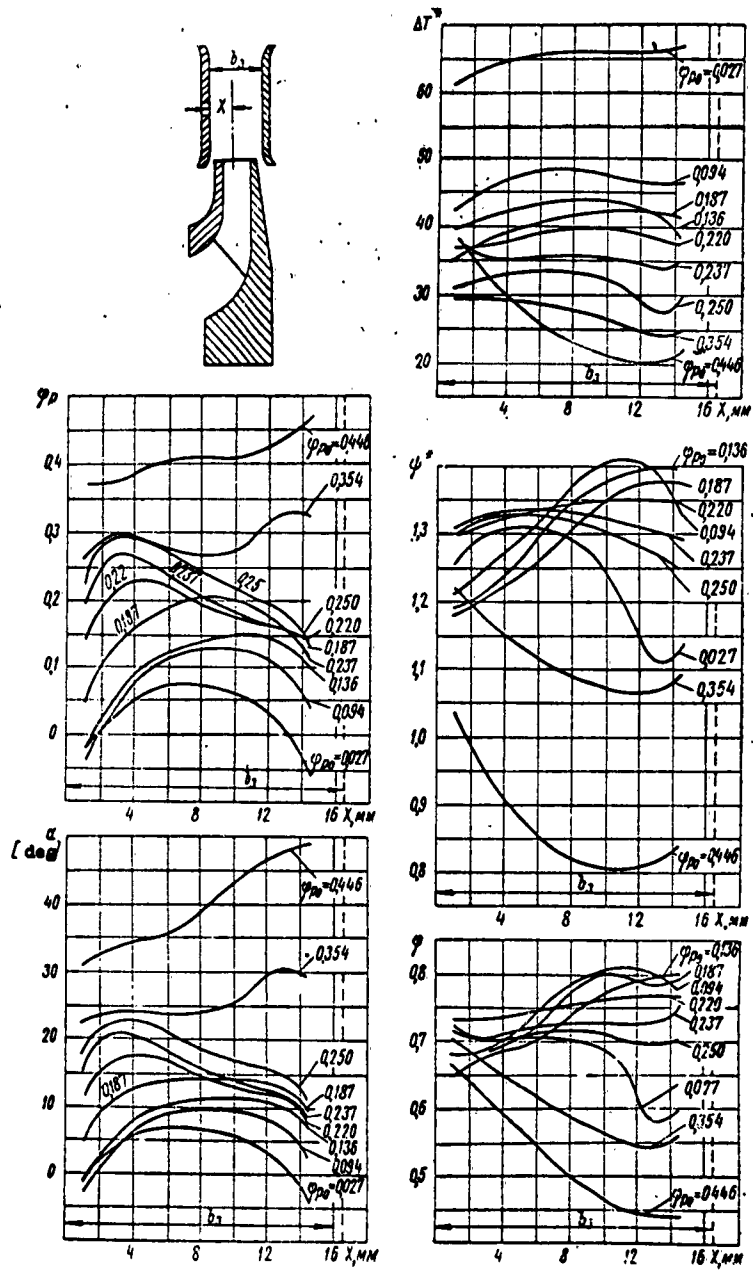


Fig. 4. Flow structure behind the wheel.

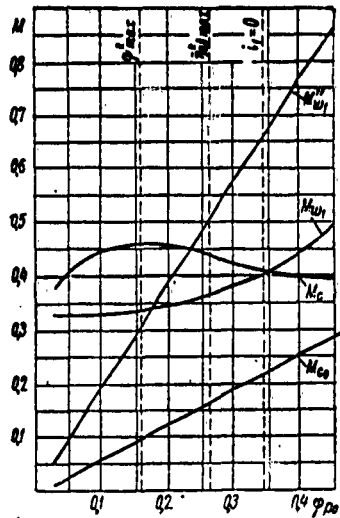


Fig. 5. Characteristics of the wheel according to number M ($z_1 = z_2 = 16$).

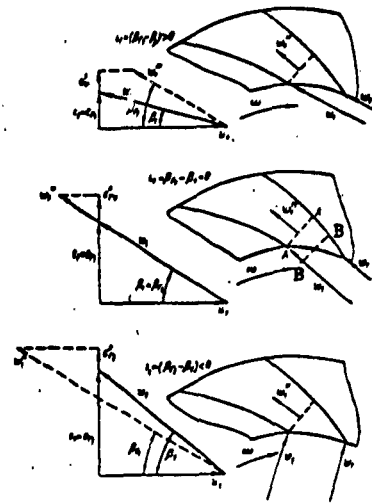


Fig. 6. Inlet velocity triangles of a centrifugal wheel with and without taking into account the restriction and bending of the flow.

REFERENCES

1. F. S. Rekstin. Stend ETsK-1 laboratorii kompressornykh mashin LPI im. M. I. Kalinina. Nauchno-tekhnicheskiy informatsionnyy byulleten', LPI, 1959, No. 6.
2. Yu. S. Podobuyev and K. P. Seleznev. Teoriya i raschet osevykh i tsentrobeznykh kompressorov. Mashgiz, 1957.
3. S. P. Livshits. O vliyani zakrutki potoka i uglov ataki pri vkhode v rabocheye koleso tsentrobeznoho kompressora. Energo-mashinostroyeniye, 1958, No. 12.

THE INFLUENCE OF THE NUMBER OF VANES ON THE EFFICIENCY
OF THE CENTRIFUGAL WHEEL WITH A SINGLE-STAGE CASCADE

S. A. Anisimov, F. S. Rekstin, and K. P. Seleznev

The operating efficiency of a wheel depends on the type, the relative dimensions, and the operating regime of the wheel. In addition to the M and Re numbers and the angle of attack i_1 (or φ_{p_0}) for a given medium with a specific heat ratio k , the basic parameters which define the operation of the wheel are the geometric characteristics β_{g_2} , b_2/D_2 , Z_2 , β_{g_1} , D_1/D_2 , D_0/D_2 , F/F_0 , the shape of the vane profile, and others.*

In this article we analyze the results of an experimental study of the influence of the number of vanes of a centrifugal wheel on its characteristics and on the flow structure behind it. The work was conducted on the ETsK-1 test stand at the Compressor Machine Laboratory of the Kalinin Leningrad Polytechnic Institute.

The diagram of the blading of the stand is shown in Fig. 2 on p. 16.

The tests were conducted using ten shrouded wheels with entirely

* The arbitrary designations used in this article are, with very few exceptions, the generally-accepted ones.

milled vanes having an angle $\beta_{g_2} = 49^\circ$. The wheels differed only in the number of vanes: $z = z_1 = z_2 = 4, 6, 8, 10, 12, 14, 16, 20, 24,$ and 28. The basic geometric parameters of these wheels have been given in a previous article [1]. The diffusivity of the channels and the wheel $F_2'/F_1', F_1''/F_1''$ and F_2''/F_1'' , the relative pitch of the equivalent straight cascade t/l , the coefficients of flow restriction by the vanes, and the angles of exposure of the inter-vane channels in the plane of rotation at the inlet τ_1 and ν_1 , and at the outlet τ_2 and ν_2 , for a series of test wheels are given in Fig. 1. Here,

$$\tau_1 = \frac{F_1'}{F_1} = \frac{\pi D_1 b_1 - z_1 b_1 \frac{\delta_1}{\sin \beta_{g_1}}}{\pi D_1 b_1} = 1 - \frac{\delta_1 z_1}{\pi D_1 \sin \beta_{g_1}}; \quad (1)$$

$$\tau_2 = \frac{F_2'}{F_2} = \frac{\pi D_2 b_2 - z_2 b_2 \frac{\delta_2}{\sin \beta_{g_2}}}{\pi D_2 b_2} = 1 - \frac{\delta_2 z_2}{\pi D_2 \sin \beta_{g_2}}; \quad (2)$$

$$\frac{t}{l} = \frac{2\pi \sin\left(\frac{\beta_{g_1} + \beta_{g_2}}{2}\right)}{z \ln \frac{D_2}{D_1}}; \quad (3)$$

$$\frac{F_2''}{F_1''} = \frac{F_2 \tau_2 \sin \beta_{g_2}}{F_1 \tau_1 \sin \beta_{g_1}} = \frac{F_2'}{F_1'} \cdot \frac{\sin \beta_{g_2}}{\sin \beta_{g_1}}; \quad (4)$$

$$\nu_1 = \frac{360}{z_1} \left(1 - \frac{D_1}{2R_1} \cos \beta_{g_1}\right); \quad (5)$$

$$\nu_2 = \frac{360}{z_2} \left(1 - \frac{D_2}{2R_2} \cos \beta_{g_2}\right). \quad (6)$$

where

$$R_1 = \frac{R_2^2 - R_1^2}{2(R_2 \cos \beta_{g_2} - R_1 \cos \beta_{g_1})}.$$

From the graphs in Fig. 1 it follows that when $z = 4-28$ the coefficients $\tau_1 = 0.91-0.39$ and $\tau_2 = 0.97-0.78$ (when $z = 16$, $\tau_1 = 0.66$ and $\tau_2 = 0.87$). As can be seen from these numbers, the investigated wheels had great restriction, which is characteristic of limited-performance centrifugal wheels. For comparison, we give the values of τ for the same type of wheel on two machines of the Neva Machine-Construction Factory: the K-100-61-1; $\tau_1 \approx 0.73$, $\tau_2 \approx 0.87$, and K-500-61-1; $\tau_1 \approx 0.73-0.76$, $\tau_2 \approx 0.89$.

1. The Problem

In solving the problem of selection of the best number of vanes for the wheel we are usually guided by the following concepts. As is known [3, 4, 5], the theoretical head h_T which the gas attains in the wheel channels when $c_{u_1} = 0$ is determined from the formula

$$h_T = \frac{c_{u_2} u_2}{g} = \varphi_2 \frac{u_2^2}{g}, \quad (7)$$

where $\varphi_2 = c_{u_2}/u_2$.

Using as our basis the Stodola formula, which is often used in the theory of stationary centrifugal compressors to calculate the influence of finite number of vanes, we get

$$\varphi_2 = 1 - \frac{\pi}{z_2} \sin \beta_{2s} - \frac{c_{r_2}}{u_2} \cot \beta_{2s}. \quad (8)$$

From this it follows that with increasing z_2 there is an increase in φ_2 and, consequently, in h_T . In deriving Formula (8) we took into account only the effect of the relative eddy on the velocity value c_{u_2} because of the finite number of vanes.

However, with the flow of a real gas in a centrifugal wheel with a finite number of vanes, in addition to the action of the relative eddy, there are a number of other factors which influence the velocity triangle and, consequently, the value of φ_2 .

With a considerable reduction in z the load on each vane increases, the pressure and velocity gradients are raised on the surface of the vane, and the intensity of the diffuser zone on the profile increases. There is a simultaneous increase in the angle of exposure of the inter-vane channel and local values of the Mach number. These all result in the appearance and development of separation zones which disrupt flow in the channel, cause a decrease in the head due to

decreased lifting force and, as a result, additional deviations in the flow at the outlet, and also lead to decreased efficiency. The separation zones restrict the outlet cross section, increase the flow velocity, and, consequently, decrease the coefficient ϕ_2 according to Formula (8). From what has been said it is clear that with a small number of blades the head will decrease more sharply than follows from theoretical relations (7) and (8).

On the other hand, with an increased number of blades their surface greatly increases, i.e., frictional losses increase, which results in a drop in the useful head and the efficiency of the wheel. There is simultaneously increased diffusivity of the wheel channel (see Fig. 1) and a great increase in the gas velocity at the inlet to the channel due to sharp restriction of the flow (small τ_1 values). These factors also cause the development of separation zones and, as a result, a decrease in the theoretical and useful heads.

From what has been said it is clear that the head and the efficiency of the wheel should be maximum for some average number of vanes.

Another important parameter which determines the efficiency of the wheel is the width of the operating zone of the characteristic.

Let us examine this question for the case of the flow of an ideal gas. Theoretical investigations have shown [3, 4] that under specific conditions (an inviscid gas, unstressed entry, low output) the gas velocity w on the working side of the blade (the side facing the flow), because of the influence of the relative eddy, can drop to zero or even become negative. This latter will indicate the appearance of inverse flows on the acting surface of the vane and, consequently, unstable gas motion. Such flow motion causes the appearance of an eddy region. The output V_{cr}^1 at which the gas velocity w on the

acting surface of the blade decreases to zero determines the boundary of stable wheel operation and is called the critical output. This output is associated with the optimum output V'_{opt} by the following relation [4]:

$$\frac{V'_{cr}}{V'_{opt}} = \frac{2\pi r \sin^2 \beta_2}{\left(1 + \frac{\bar{a}}{2R_1}\right) k_2 \frac{c_r}{u} z} \quad (9)$$

where \bar{a} is the width of the vane channel in the wheel revolution plane.

From this formula it follows, in particular, that with an increased number of vanes V'_{cr}/V'_{opt} decreases, i.e., the acting zone of the characteristic increases. However, the flow structure of an ideal gas in a wheel in a design and nondesign regime, as experimental studies have shown, differs considerably from the theoretical structure [3, 4]. This is manifested, in particular, by the fact that inverse flow does not occur along the acting side of the vane, even with very low outputs. And, conversely, on the nonacting side of the vane there is always breakaway, which is the more noticeable the lower the output. These facts make it necessary to use with care those conclusions from Formula (9) dealing with the influence of the number of vanes on the value of the acting zone of the characteristic. The difference between the actual flow pattern and that of an ideal gas is explained by the appearance of separation in the boundary layer on the diffuser segments of the nonacting surface of the vanes and by their development, which results in increased average relative velocity \underline{w} .

Finally, an increase in z obviously complicates the design and construction of the wheels, i.e., it increases their cost.

The relation between the actual flow structure in the wheel channels and the number of vanes, as is clear from the preceding, is extremely complex and, at least at present, has not been precisely

determined theoretically. Thus the problem of selecting the number of vanes should be solved by taking into account theoretical and experimental data. For practical purposes, the number of vanes should be selected depending on which wheel characteristics are used as the determining ones, viz., efficiency, head, width of acting zone of the characteristic, flow structure behind the wheel, reliability, feasibility, etc. This latter results from the fact that at present it is actually impossible to create a wheel to satisfy simultaneously all these various requirements. In other words, a wheel may be optimum only with respect to certain characteristics. This is the difficulty in selecting the number of vanes and; in general, the arbitrary nature of this concept.

In stationary centrifugal compressors in the past, the wheels were made with a relatively large number of vanes ($z \geq 28$). At present, fewer vanes are used. For example, at the Neva Machine-Construction Factory, for typical "compressor" ($\beta_{g_2} = 45^\circ$ and $c_{r_2}/u_2 = 0.24$) and "pump" ($\beta_{g_2} = 20^\circ$ and $c_{r_2}/u_2 = 0.12$) wheels, 18 and 8 vanes, respectively, are used [6].

Various analytical dependences are used in the literature to select the appropriate number of vanes. These dependences, and also the results of using them to calculate the recommended number of vanes for the wheels we investigated, are given in the table. As can be seen from the table, the recommended number of vanes varies within a rather broad range - from 8 to 23 - depending on which formulas were used in the calculations.

The experimental data in Soviet and foreign literature on the influence of the number of vanes of a centrifugal wheel on its characteristics are incomplete and pertain to studies of wheels which are

not typical for stationary centrifugal compressors [7, 14], or to determination of the total characteristics of centrifugal stages with wheels having various z [15]. The literature contains no detailed data on the influence of the number of vanes on the flow structure behind the impeller.

2. Research Methods

The method of investigating the influence of the number of vanes of a wheel on the efficiency of its operation is based mainly on the method of investigating the operation of individual wheels given in previous papers [1, 2]. The main difference is that if when investigating individual wheels, as an independent parameter we use φ_{p_0} or X , then when investigating the influence of the number of vanes it is natural to use, as the independent parameter, the number of vanes and also the coefficient τ_1 , the relative pitch t/l , and the angle of exposure of the vane channel ν_1 , uniquely associated with z for the investigated wheels and giving a more complete idea of the conditions of flow entry into the wheel channels. In addition to the previously used criterional parameters (see the footnote on p. 3) $\bar{\eta}_{a\partial}^*$, ψ^* , φ , Ω , ρ , k_G , k_α , etc., to investigate the influence of the number of vanes on the width of the acting zone of the characteristic of the wheel we introduced the auxiliary criterional parameter, the coefficient k_y :

$$k_y = \frac{\varphi_{p_0, \text{opt}} - \varphi_{p_0, \text{cr}}}{\varphi_{p_0, \text{cr}}}, \quad (10)$$

where $\varphi_{p_0, \text{cr}}$ and $\varphi_{p_0, \text{opt}}$ are the gas flow factors φ_{p_0} for ψ_{max}^* and $\bar{\eta}_{a\partial}^* \text{ max}$, respectively.

When k_y increases there will be expansion of the acting zone of the wheel characteristic.

3. Investigation Results

1. The curve $\eta_{ad}^* \max$, shown in Fig. 2, is smooth for a broad range of z ($z = 8-20$).

When $z < 8$ there is a noticeable drop in the efficiency due to deterioration of the flow structure in the wheel channels, associated with separation phenomena. With such a small number of vanes the load evidently increases greatly on the vane, and the exposure angle of the vane channel increases considerably, which results in the vigorous development of separation phenomena. In this case, in the vane channels there occur local pressure and velocity gradients.

When $z > 20$ there is a certain decrease in the efficiency due to the strong restriction of the flow at the inlet (the velocity w_1'' and the number M_{w_1}''), an increase in the diffusivity of the channels and the wheel (F_2'/F_1'' , F_2/F_1' , and F_2''/F_1'' increase), and the influence of friction.

The maximum η_{ad}^* is in the region $z = 10-18$. In this case the angles of attack are within the limits $i_1 \approx 3-7^\circ$.

The numerical value of the angle of attack depends on the shape of the leading edge of the profile. The angle of attack is calculated from the angle β_{g_1} which is determined by the direction of the camber line at radius R_1 , while the leading edge of the blade is practically symmetrical. Depending on the shape of the leading edge, optimum flow can occur for several values of i_1 . For example, with tapering of the leading edge of comparatively thick completely-milled vanes from the concave side, unstressed flow will be attained at $i_1 > 0$.

In addition, we should bear in mind the influence on the true value of the angle of attack of leakages near the covering disk, although their influence is quite insignificant and is, on the average,

for the examined wheels (radial gap of 0.25-0.35 mm) in optimal regimes $\Delta i_1 \leq 30-40'$. The leakages decrease the algebraic value of the angle of attack.

The above phenomena have remained practically unstudied; therefore it is very difficult to estimate the actual extent of the influence of these factors. Special experimental and theoretical operations are required to solve these problems.

2. The shape of the curves $\psi_{\max}^* = f(z)$ and $\varphi_{\max} = f(z)$ shown in Fig. 2 is similar to that of the curve $\bar{\eta}_{a\partial \max}^* = f(z)$. The decrease in the value of ψ_{\max}^* and φ_{\max} with small and large z can be explained by the same reasons as the decrease in $\bar{\eta}_{a\partial \max}^*$. The maximum ψ^* and φ are in the region $z = 14-20$.

3. Figure 3 gives individual characteristics of wheels with various numbers of vanes. From the graphs it follows that since the curves $\bar{\eta}_{a\partial}^*$ and ψ^* are more sloping with decreasing number of vanes, consequently with decreasing z the zones of economical and stable wheel operation increase.

The increased zones of economical and stable operation with decreasing number of vanes can evidently be explained as follows. When $i_1 \approx 0$ flow past the leading edges is not characteristic; the wheel characteristics are determined by conditions of gas flow in the wheel channel. When $i_1 \neq 0$ and their absolute values are reasonably high, the maximum local M numbers and maximum local diffusivity occur with gas flow near the leading edges. The nature of the flow past these edges for any z should evidently be similar, since for all the investigated wheels their shape is identical, while the value of maximum diffusivity and the maximum M number in this region should be determined mainly by the average value of the M number near the

leading edges. From the graph in Fig. 6 we see that with an increase in \underline{z} the number M''_{w_1} continually increases, i.e., with an increase in \underline{z} breakaways begin to develop at lower absolute values of the angles of attack than we observed in the investigated wheels.

With an increase in \underline{z} the efficiency maxima shift toward smaller φ_{p_0} , while the head coefficient maxima, on the other hand, shift toward higher φ_{p_0} , i.e., in this case we observe a certain decrease in $\varphi_{p_0 \text{opt}}$ and an increase in $\varphi_{p_0 \text{cr}}$. This indicates that with an increasing number of vanes the width of the acting zone of the wheel characteristic defined by the coefficient k_y (Fig. 2) decreases. This latter does not confirm theoretical formula (9).

The shift in the maxima of $\eta_{a_0}^*$ and ψ^* vs. \underline{z} can evidently be explained by the influence exerted by the change in the value of flow constriction at the inlet on the ratio between M''_{w_1} and $M''_{w_1 \text{cr}}$.

The critical number $M_{w_1 \text{cr}}$ is the value of M_{w_1} at which at any point on the surface of the profile the gas velocity attains the local velocity of sound. The value of $M_{w_1 \text{cr}}$ depends basically on the geometry of the cascade design and the angle of attack. To assure normal operation of the cascade we must have the inequality $M_{w_1} \leq M_{w_1 \text{cr}}$. Otherwise, on the vane surface there arises a supersonic zone and, as a result, there are compression shocks which cause the vigorous development of breakaway phenomena and a sharp deterioration of the flow aerodynamics in the wheel channels.

The value of the local velocity in the vicinity of the leading edge depends mainly on the shape of the edge, the angle of attack, and the value of the velocity ahead of the cascade and in the throat of the cascade channel. The local velocity for the given geometry and specific velocity ahead of the cascade is minimum when $i_1 \approx 0$

and increases when $i_1 \neq 0$. For the given angle of attack the local velocity increases with increasing constriction, i.e., with increasing z (except for the case of very small z) due to increased velocity in the narrow channel cross section.

There are practically no data on the value of $M''_{w_1 cr}$ for circular cascades. In this article let us give an analysis, using the concept of the critical number $M''_{w_1 cr}$, by which we will understand that M''_{w_1} number [1] for which somewhere on the profile there occurs a local velocity equal to the local velocity of sound.* The number $M''_{w_1 cr}$ has a maximum value at $i_1 \approx 0$ and decreases when $i_1 > 0$ and $i_1 < 0$.

Regimes corresponding to $\eta_{a0}^* \max$ lie in the region of small angles of attack close to zero. In this case there are optimum conditions for vane profile flow, due to which the number $M''_{w_1 cr}$ has a high value and changes but little with slight changes in the angle of attack, i.e., in this case preservation of the inequality $M''_{w_1} < M''_{w_1 cr}$ will depend mainly on the change in the value of M''_{w_1} and, consequently, with constant cascade geometry, only on the value of the coefficient φ_{p0} .

Let us write the expression

$$M''_{w_1} = \frac{w_1}{\sqrt{kgRT_1}} = \frac{\sqrt{c_{r_1}^2 + u_1^2} \frac{\sin \beta_1}{\tau_1 \sin \beta_{g1}}}{\sqrt{kgRT_1}} = \frac{c_{r_1}}{\tau_1 \sin \beta_{g1} \sqrt{kgRT_1}} \quad (11)$$

From this it follows that with increasing velocity c_{r_1} and, consequently, φ_{p0} , and with increasing flow restriction (i.e., with decreasing τ_1), the velocity w_1'' and the number M''_{w_1} will increase.

* The critical number $M''_{w_1 cr}$ should be considered arbitrary, since for not very high u_2 and small or average values of z it is possible that local supersonic velocity is not attained. In this case, $M''_{w_1 cr}$ characterizes the regime for which due to high local diffusivity breakaways vigorously develop.

Thus the influence of the flow rate and flow restriction on M''_{w_1} is qualitatively identical. Or, in other words, in order that the number M''_{w_1} not change with increasing restriction due to an increase in the number of vanes it is necessary that the gas flow rate (i.e., φ_{p_0}) decrease. Therefore, in the regimes $\eta_{ad}^* \rightarrow \max$, when preservation of the inequality $M''_{w_1} < M''_{w_2 cr}$ depends mainly on the value of M''_{w_1} , with increasing z there must be decreased gas flow to prevent an increase in M''_{w_1} . From this it is understandable that with increasing z the coefficient $\varphi_{p_0 opt}$ should decrease.

Regimes corresponding to ψ_{max}^* lie in the region of large positive angles of attack and have correspondingly poor conditions of vane profile flow, due to which the number $M''_{w_1 cr}$ has a relatively low value and depends greatly on the angle of attack, i.e.; in this case with constant cascade geometry preservation of the inequality $M''_{w_1} < M''_{w_1 cr}$ will be determined mainly by the value $M''_{w_1 cr}$, which changes abruptly even with insignificant changes in the angles of attack or φ_{p_0} . Increased flow rate in this case leads to a decrease in i_1 and therefore causes a considerable increase in $M''_{w_1 cr}$. In this case there is also a certain increase in M''_{w_1} ; however, we must assume that an increase in the flow factor influences an increase in the number M''_{w_1} to a much lesser extent than an increase in $M''_{w_1 cr}$, i.e., the inequality $M''_{w_1} < M''_{w_1 cr}$ is retained. With decreasing flow rate, i.e., an increase in the angles of attack, the opposite should be observed. In this event the inequality $M''_{w_1} < M''_{w_1 cr}$ is not preserved.

Thus, in regimes ψ_{max}^* when the decisive factor is $M''_{w_1 cr}$, retention of the inequality $M''_{w_1} < M''_{w_1 cr}$ with increasing z (and, consequently, the number M''_{w_1}) is possible only when the flow rate changes such that the number $M''_{w_1 cr}$ increases. This will occur with a decrease in the

angle of attack, i.e., with an increase in φ_{p_0} [1]. From this we see that with increasing z the coefficient φ_{p_0} corresponding to ψ_{\max}^* , i.e., $\varphi_{p_0 \text{ cr}}$, should increase, which is confirmed by experimental data obtained (see Figs. 2 and 3).

In addition, from Formula (11) it follows that the qualitative influence of u_1 on the number M_{w_1}'' when $i_1 = \text{const}$. i.e., when $\sin \beta_1 / \sin \beta_{g_1} = \text{const}$, is opposite to the influence of τ_1 ; therefore we can assume that for wheels similar to those investigated an increase in the velocity u_1 , when its value is reasonably high, should cause qualitatively the same type of shift of the maxima of $\eta_{a\delta}^*$ and ψ^* as a decrease in τ_1 , i.e., an increase in the number of vanes z . In other words, to expand the acting zone of the wheel characteristic we must decrease the peripheral velocity of the wheel u_1 . This latter conclusion naturally requires experimental verification.

A change in the angle β_{g_1} , when the remaining geometric parameters of the wheel are retained, results in a change in the optimum flow rate, i.e., the optimum value of the coefficient φ_{p_0} . Using wheels with large β_{g_1} it is evidently possible to displace the zone of maximum efficiency to the region of increased flow rates.

The results obtained on the shift in the maximum of the curves $\psi^* = f(\varphi_{p_0})$ with a change in z agree with the experimental data of Kearton [14] and Ris [15]. The shift in the maximum of the curves $\bar{\eta}_{a\delta}^* = f(\varphi_{p_0})$ does not agree with the experimental data of these authors; this latter can evidently be explained by the influence of the fixed elements, since our data pertain to a wheel, while the other data [14, 15] correspond to a stage and a unit, respectively.

4. The coefficients of relative flow nonuniformity with respect to the internal k_{h_1} and adiabatic $k_{h_{a\delta}}^*$ heads (Figs. 4 and 5) are

practically independent of the number of vanes, both for $\eta_{ad}^* \max$ and $i_1 = 0$, and for ψ_{\max}^* .

The relative flow nonuniformity with respect to flow rate and angle, characterized respectively by the coefficients k_G and k_α (Figs. 4 and 5), depends on z , particularly for ψ_{\max}^* . This is associated with the fact that the operational regimes corresponding to ψ_{\max}^* lie close to the surge zone where breakaway phenomena are particularly greatly manifested.

For regimes $\eta_{ad}^* \max$ and $i_1 = 0$ a certain increase in k_G and k_α is observed with a decrease of $z < 8$, due to the development of breakaway phenomena because of increased load on the blades and increased velocity and pressure gradients, and with an increase in $z > 14$, due to the increased diffusivity of the channels and the wheel and also increased friction in the channels.

The absolute nonuniformity with respect to the angle $\Delta\alpha = \alpha_{\max} - \alpha_{\min}$ (Figs. 4 and 5) when $z = 10-20$ is minimum and remains practically constant, but increases considerably when $z \leq 8$. In our test wheels the absolute nonuniformity with respect to the angle was $6-10^\circ$, i.e., the variation of the angle α about the average value was $\pm(3-5)^\circ$ even for the regimes $\eta_{ad}^* \max$ and $i_1 = 0$. The presence of a considerable absolute nonuniformity with respect to the angle even for design regimes should be taken into consideration when designing vaned diffusers and particularly for the shape of the leading edges of the vanes.

5. The nature of the change in the degree of reaction Ω with a change in z is determined basically by the nature of the change in ϕ [1], while the degree of reaction ρ is determined, in addition, by energy losses (Fig. 4).

The values of Ω and ρ decrease greatly with an increase in z to 6-8. With a further increase in z the decrease in Ω and ρ occurs considerably more slowly (when $\eta_{ad}^* \max$ and $i_1 = 0$), while for ψ_{\max}^* the values of Ω and ρ in this region remain practically constant. For all numbers of vanes, as follows from the theory $\Omega > \rho$ [1].

6. A comparison of the curves $\varphi = f(z)$ and $\varphi_c = f(z)$ [1]* for $\eta_{ad}^* \max$ (Fig. 4) and also for $i_1 = 0$ shows that they are qualitatively identical, but the numerical value of φ_c is less than the experimental value of φ . With an increase in z the values of φ_c and φ converge. These data agree with those derived by Kearton [14].

7. The dependence of the numbers M_{c0} , M_{w1} , M_{w1}'' and M_c on the number of vanes for $\eta_{ad}^* \max$, $i_1 = 0$, and ψ_{\max}^* is shown in Fig. 6. The nature of the curves of M_{c0} and M_{w1} is determined by the change in the coefficient φ_{p0} corresponding to the regimes $\eta_{ad}^* \max$, $i_1 = 0$ and ψ_{\max}^* for various z . The nature of the curve M_c for all regimes is determined by the influence of the number of vanes on φ and Ω [1]. The value of M_c with increasing z basically increases, most intensely in the region $z = 4-10$, and very slowly for $z > 14-16$.

When $i_1 = 0$ the number M_{w1}'' continually increases with increasing z , since restriction increases (τ_1 decreases). For ψ_{\max}^* the value of M_{w1}'' with increasing z increases considerably due to increased restriction as well as due to the shift of ψ_{\max}^* to the region of high flow rates, where effusivity increases at the cascade inlet.

The value of M_{w1}'' for $\eta_{ad}^* \max$ in the region $z \leq 16$ remains approximately constant. This constancy of the value of M_{w1}'' with a change

* The coefficient $\varphi_c = c_u/u_2$ is found by converting from diameter D_2 to the diameter of the control section D of the coefficient $\varphi_2 = c_{u2}/u_2$ defined by the Stodola formula.

in the number of vanes in the region $z \leq 16$ for $\eta_{a\partial}^* \max$ supports the previously expressed concepts on the influence of the number M_{w_1}'' on the position of the maximum efficiency. With a further increase in the number of vanes, preservation of the constancy of M_{w_1}'' would result in a great reduction in the flow rate and a great increase in the angle of attack, in which case the number $M_{w_1 cr}''$ would noticeably decrease. Therefore the maximum efficiency for $z \geq 16$ is attained for approximately constant angles of attack corresponding to the regime in which $M_{w_1 cr}''$ is still large and approximately equal to its value when $i_1 = 0$. For somewhat larger angles of attack the value of $M_{w_1 cr}''$ will evidently decrease considerably. It is characteristic that when $z > 16$ $\eta_{a\partial}^* \max$ begins to gradually decrease, which is evidently associated with an increase in M_{w_1}'' , and which supports our conclusions.

The coefficient $\varphi_{p_0 M}$ (the flow factor φ_{p_0} , for which $w_1 = w_1''$) decreases with increasing restriction due to increasing z , as can be seen from Fig. 6. Thus, with an increase in the number of vanes the transition point from a diffusion zone to an effusion zone shifts toward lower flow rates. Or, in other words, with increasing z the region of operational regimes for which there is diffusion inlet into the vane channel of the wheel decreases.

Conclusion

1. Our studies have permitted a qualitative and quantitative estimate of the influence of the number of vanes z on the operational efficiency of a wheel. Obviously, however, the specific quantitative data on the influence of the number of vanes (e.g., the number of vanes corresponding to maximum efficiency) are relative in nature.

This is due to the fact that the wheel efficiency depends on many factors, and therefore quantitative data, strictly speaking, are valid only for specific design relationships for a wheel, and for the gas-dynamic flow parameters, i.e., for specific β_{g_2} , β_{g_1} , D_1/D_2 , δ/D_2 , u_2 , the shape of the leading edge of the vanes, etc. Some change in these parameters (e.g., the thickness of the vanes δ) compared with those used in the studies could obviously have the result that the influence of z would change quantitatively (e.g., the maximum efficiency would occur for some other number of vanes).

We should, however, note that this study was conducted for wheels made according to the generally-accepted recommendations for typical wheels of stationary low-output centrifugal compressors. This fact increases the value of the obtained quantitative relationships.

In addition, the above analysis makes it possible to draw certain conclusions as to the influence of the number of vanes on the physical flow pattern in a circular cascade.

Thus, analysis of the obtained experimental data makes it possible, in many cases, to give a qualitative (and in a number of cases a quantitative) estimate of the influence of z for other design and gasdynamic parameters of the wheel and the flow.

In thus recommending that the above data be used in practice, the authors at the same time consider that the above given theoretical analysis should now be further refined, and special experimental operations should be undertaken.

2. To investigate shrouded wheels with normally backward bent vanes (in the given case, $\beta_{g_2} = 49^\circ$), the curves $\eta_{ad}^* \max$ and ψ_{\max}^* as functions of z have a sloping nature for a broad range of vane numbers. Therefore the maximum efficiency of the head coefficient is found for

a broad range of vane numbers $z \approx 10-20$ (for the head, $z \approx 14-20$; for the efficiency, $z \approx 10-18$). We should note that the restriction of the channel at the inlet to the investigated wheels was considerable (when $z = 10-20$ $\tau_1 = 0.78-0.57$) because of the large relative thickness of the milled vanes ($\delta_1/D_1 = 0.0345$). These relations with respect to τ_1 and δ_1/D_1 are characteristic of low-output centrifugal compressors. For wheels with a smaller relative vane thickness δ_1/D_1 (for stamped vanes $\delta_1(1 + (2\Delta/b_1))/D_1$, where Δ is the length of the flange) we can expect to obtain maximum efficiency and head coefficients for somewhat more vanes.

Such an assumption can be made with respect to wheels having an angle β_{g_1} which is larger than that of the investigated wheels.

3. The number of vanes greatly influences the value of the zone of stable and economic wheel operation regimes and, consequently, the width of the acting zone of the characteristic. With an increase in z the position of the efficiency maximum shifts toward the region of lower flow rates, while the maximum head coefficient shifts toward the region of lower flow rates, while the maximum head coefficient shifts toward the region of higher flow rates and thus the acting zone of the characteristic is greatly reduced. In this regard, to increase the acting zone of the characteristic as small a number of vanes z as possible must be selected.

With large z , when there is great restriction of the flow by the vanes, the acting zone of the characteristic can evidently be expanded if we undercut every other vane, since this should increase τ_1 and, consequently, decrease M_{w_1}'' .

4. The most satisfactory flow structure behind the wheel, as the results of our tests on the series of wheels showed, is obtained for $z = 10-20$.

For wheels with $z = 10-20$ the absolute nonuniformity, with respect to the angle, of the flow behind the wheel remained practically constant. In this case the deviation of the flow angle from the average value was $\pm(3-5)^\circ$ ($\Delta\alpha = \alpha_{\max} - \alpha_{\min} = 6-10^\circ$) at a distance of 6.5 mm behind the wheel. This should be taken into consideration when designing vaned diffusers.

5. The angles of attack in regimes of maximum efficiency were within the limits $i_1 = 3-7^\circ$ when $\tau_1 = 0.78-0.57$ ($z = 10-20$).

6. Comparison of the magnitudes and nature of the change in the M_c and M_{w_1}'' numbers (with a change in φ_{p_0} , z , τ_1) resulted in the conclusion that the number M_c (more exactly the number M_{c_2}) is not a characteristic criterion of the operation of the wheel, but can serve primarily as a characteristic of the operating conditions of the diffuser. The criterion which determines the operation of the wheel is the number M_{w_1}'' or other numbers which are determined by the inlet velocity. Therefore there must be theoretical and experimental studies to establish the critical values of M_{w_1}'' and M_{w_1} for characteristic designs, and these must be used as the criteria when selecting the maximum permissible peripheral velocities.

In testing the indicated series of wheels for $u_2 = 215$ m/sec in the region $z = 10-18$, where the maximum values of $\eta_{ad}^* \max$ were obtained, the value of M_{w_1}'' was within the limits 0.5-0.53 ($M_c = 0.41-0.44$).

Thus, for wheels similar to those investigated $z = 14-18$ should be considered the best number of vanes, from the standpoint of obtaining maximum efficiency and head and satisfactory flow structure behind the wheel. If there are rigid requirements for the value of the acting zone of the wheel characteristic, $z = 10-12$ should be considered to be

the best number of vanes. For the investigated wheels the experimental data show that the formulas proposed by a number of authors [6, 7, 12, 13] give quite accurate results for finding the optimum number of vanes with respect to efficiency and head. However, for a proper selection of the number of vanes, taking into account the efficiency, the head, the width of the acting zone of the characteristic, and the flow structure behind the wheel, it is necessary to use generalized experimental data.

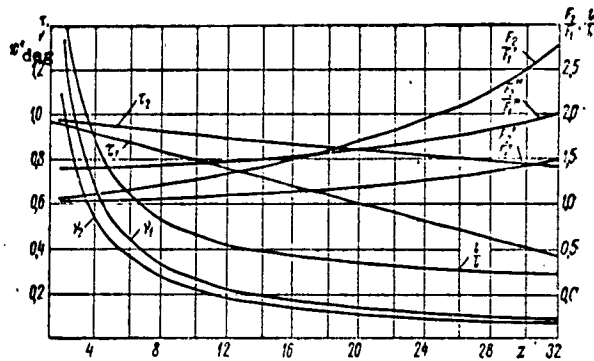


Fig. 1. Geometric parameters of the investigated wheels.

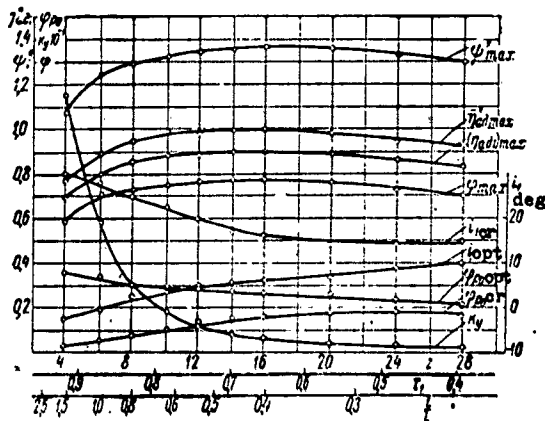


Fig. 2. Comparative characteristics of the wheels.

Optimum Number of Vanes for the Investigated Wheels
According to Various Recommendations

Author	Formula	Optimum number of vanes	Source
B. Kiderit	$z = \frac{2\pi \sin\left(\frac{\beta_{R_1} + \beta_{R_2}}{2}\right)}{\frac{l}{r} \ln \frac{D_2}{D_1}}$ $= \frac{(7.8 - 0.1) \sin\left(\frac{\beta_{R_1} + \beta_{R_2}}{2}\right)}{\log \frac{D_2}{D_1}}$ <p>Here $\frac{l}{r} = 0.35 - 0.45$</p>	18-14	[7]
V. F. Ris	$z = \frac{6.8 \sin\left(\frac{\beta_{R_1} + \beta_{R_2}}{2}\right)}{\log \frac{D_2}{D_1}}$	15-16	[6]
C. Pfeleiderer	$z = k \frac{R_2 + R_1}{R_2 - R_1} \sin \frac{\beta_{R_1} + \beta_{R_2}}{2}$ <p>The author recommends that this formula be used for centrifugal pumps. In this case, $k = 6.5$. For centrifugal compressors, $k = 11$</p>	22-23	[8, 9]
S. I. Tsitkin	$z = \frac{360}{v_1} \left(1 - \frac{R_1}{R_2} \cos \beta_{R_2}\right)$ <p>where $v_1 < 10 - 12^\circ$</p>	10-8	[10]
A. I. Stepanov	$z = \frac{\beta_{R_2}}{3^\circ}$	16	[11]
L. N. Vozilk	$z = 10 + 30D_0$ <p>where D_0 is in meters Recommended for single shrouded wheels of centrifugal compressors of transport installations</p>	18	[12]
V. N. Bilalov	$z = \sqrt{\frac{2\pi \sin \beta_{R_2}}{k}}$ $k = \frac{0.072}{2k_1} (1 + k_{v_2}) \frac{S \left(\frac{w_m}{u_2}\right)^{1/2}}{D_2^2 Re_{np}^{1/2} \left(\frac{l}{D_2}\right)^{1/2}}$ <p>Here</p> $k_1 = \frac{\pi(1 - \xi_{vm}^2)}{4k_2 k_D^2} \mu^2 \tan \beta_{R_1}$ $\xi_{vm} = \frac{D_2}{D_{out}}; k_2 = \frac{c_1}{c_0}; k_D = \frac{D_1}{D_0};$ $\mu = \frac{D_1}{D_2}; k_{v_2} = \frac{v_2}{v_1};$ $Re_{np} = \frac{D_1 u_1}{\nu_m}$ <p>S - surface of vane washed by gas; l - length of development of vane; m - average value of magnitudes between sections 1-1 and 2-2 (see Fig. 2, p. 16).</p>	19	[13]

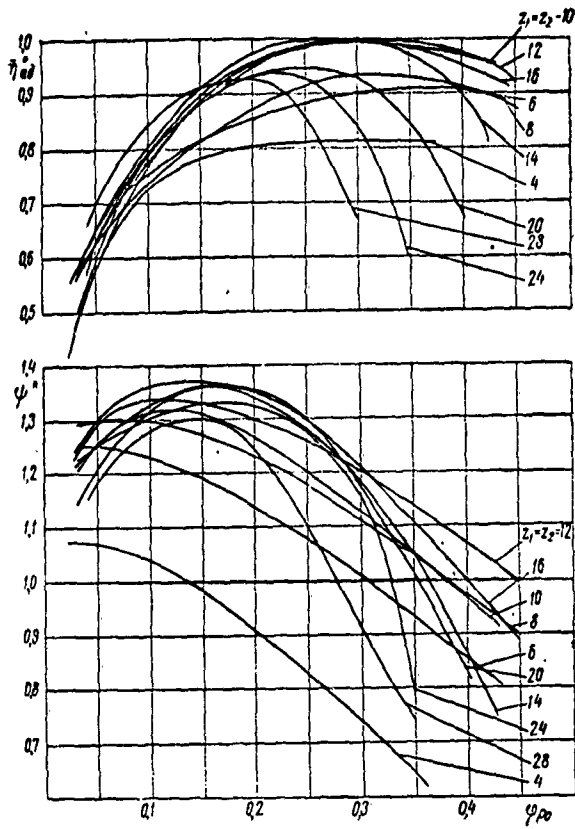


Fig. 3. Individual characteristics of wheels with various z 's.

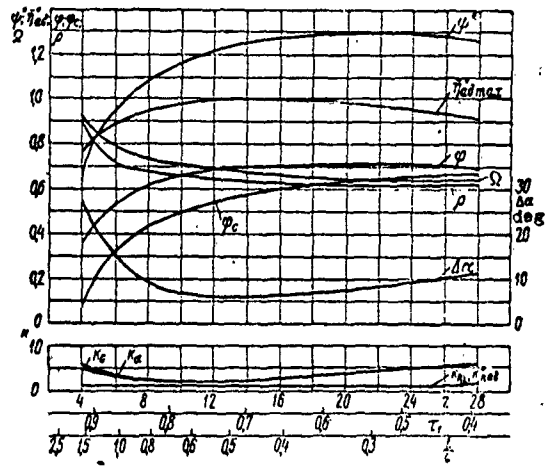


Fig. 4. Comparative characteristics of wheels for $\eta^*_{ad \max}$.

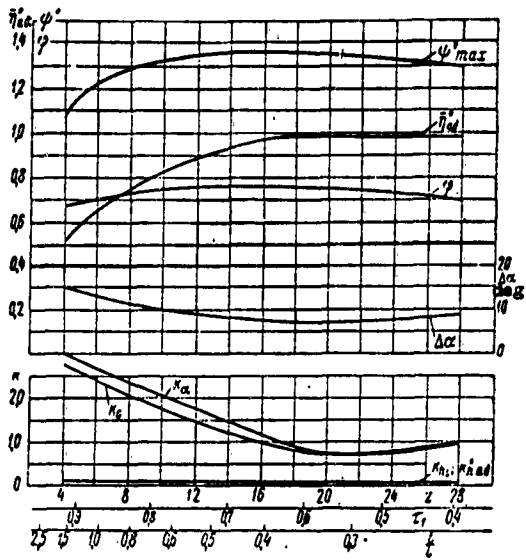


Fig. 5. Comparative characteristics of wheels for ψ_{max}^* .

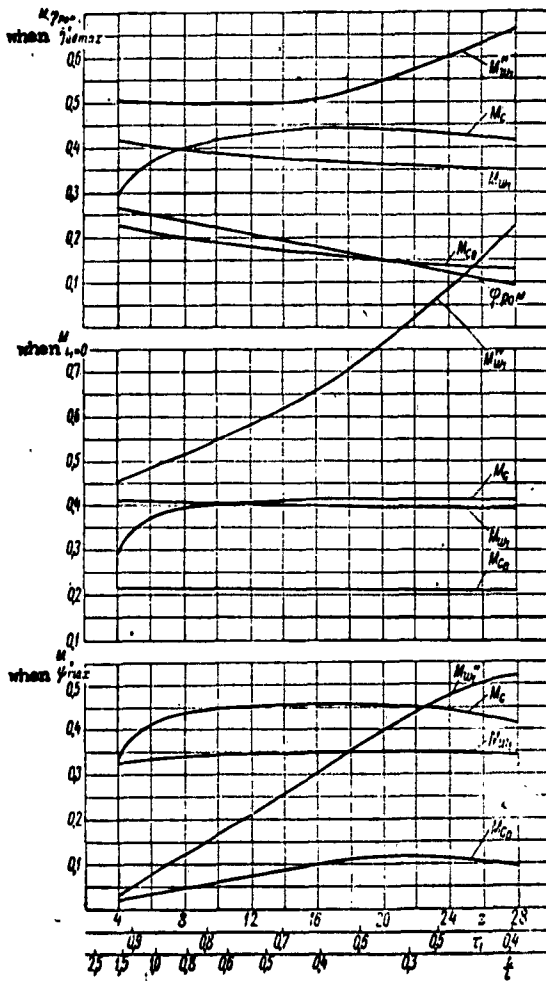


Fig. 6. Comparative characteristics of wheels for M number.

REFERENCES

1. S. A. Anisimov. [see the first article in this collection]
2. F. S. Rekstin. Stend ETsK-1 laboratorii kompressornykh mashin LPI im. M. I. Kalinina, Nauchno-tekhnicheskiy informatsionnyy byulleten' LPI, 1959, No. 6.
3. Yu. S. Podobuyev and K. P. Seleznev. Teoriya i raschet osevykh i tsentrobezhnykh kompressorov. Mashgiz, 1957.
4. V. F. Ris. Tsentrobezhnyye kompressornyye mashiny. Mashgiz, 1951.
5. K. I. Strakhovich. Tsentrobezhnyye kompressornyye mashiny. Mashgiz, 1940.
6. V. F. Ris. Kompressornyye mashiny Nevskogo mashinostroitel'nogo zavoda im. V. I. Lenina. Energomashinostroyeniye, 1957, No. 11.
7. B. Ekkert. Osevyye i tsentrobezhnyye kompressornyye. Mashgiz, 1959.
8. C. Pfleiderer. Die Kreiselpumpen für Flüssigkeiten und Gase, Berlin, 1955.
9. A. N. Sherstyuk. Kompressory. Mashgiz, 1959.
10. S. I. Tsitkin. Tsentrobezhnyye kompressory, gazoduvki i ventilyatory. Mashgiz, 1950.
11. A. I. Stepanoff. Turbobl原因ers, New York, 1955.
12. L. R. Wosika. Radial flow compressors and turbines for simple small gas turbines, Transactions of the A. S. M. E., XI, vol. 74, 1952, No. 8.
13. V. M. Kulakov. O chisle lopatok v kolese turbokompressora. Trudy MVTU im. Baumanax, 1958, No. 75.
14. W. Kearton. The influence of the number of impeller blades on the pressure generated in a centrifugal compressor and on its general performance, The Inst. of Mech. Engl. Proceedings, 1933, vol. 124.
15. V. F. Ris. Iz opyta proyektirovaniya kompressornykh mashin na NZL. Trudy NZL, 1957, Vol. I, TsBNTI.

STUDY OF THE EFFICIENCY OF CENTRIFUGAL COMPRESSOR
WHEELS WITH A TWO-STAGE VANE CASCADE

S. A. Anisimov, et al.

At the present time the stationary centrifugal compressor production industry uses wheels with a simple ($z_2 = 2z_1$) and complex ($z_2 > 2z_1$) two-stage vane cascade [1, 2, 3, 4, 5]. The guiding principles in this case are basically that such cascades can assure the required flow guidance to the outlet from the wheel with moderate restriction at the inlet.

The question of the efficiency and expediency of using wheels with $z_2 = 2z_1$ is of great practical significance, since to the present time in the literature there have been no studies made on the influence of the number of vanes and the relative diameter $\bar{D}_\kappa = D_\kappa/D_2$ (Fig. 1) on the efficiency of "compressor-type" wheels ($\beta_{g_2} = 40-50^\circ$) with a simple two-stage cascade.

These concepts also served as the basis for conducting the proposed work, a theoretical and experimental study of the influence of z and \bar{D}_κ on the operational efficiency of centrifugal wheels ($\beta_{g_2} = 49^\circ$) with a simple two-stage vane cascade. Certain data on this problem have been published previously [6].

The geometric parameters of the investigated wheels are given in Fig. 1.

1. Theoretical Study

As is known, flow in the impeller is three-dimensional. However, study of the spatial flow in the vane channels is extremely difficult. In the general case, analysis of three-dimensional flow can be replaced by separate study of two flows in the meridional and radial planes with subsequent superposition of the flow patterns one upon the other. To simplify the solution of the problem it is expedient to restrict ourselves to a study of flow only in the radial plane, taking into account the change in height of the channel b in the meridional plane. Such an assumption is possible, since usually the axial velocity component within the wheel is insignificant and has no substantial effect on the velocity profile in the vane channels.

On the basis of these concepts we conducted an approximate theoretical analysis of the influence of z and \bar{D}_κ on the operational efficiency of a centrifugal wheel, with the aim of obtaining the maximum head and minimum local M numbers in the vane channels for an optimum regime, and we also estimated the influence of these same geometric parameters on the width of the acting zone of the wheel characteristic and its hydraulic efficiency.

The useful head of the wheel can be represented as follows:

$$h_n = h_{T_\infty} - \Delta h_T - \Delta h_r,$$

where $h_{T_\infty} = 1/g(1 - (c_{r_2}/u_2)\cot\beta_{g_2})u_2^2$ is the theoretical head for an infinite number of vanes; $\Delta h_T = h_{T_\infty}$ is the decrease in the theoretical head in association with a finite number of vanes due to the influence

of the relative eddy, the curvature of the vanes, and the change in the flow structure in the channels; $\Delta h_r = h_{T_1} - h_{T_2}$ is the loss of head due to friction and vorticity.

Let us examine the dimensionless value

$$\Phi(z) = \frac{h_{T_\infty} - h_r}{h_{T_\infty}} = \frac{\Delta h_r}{h_{T_\infty}} + \frac{h_r}{h_{T_\infty}} = f_1(z) + f_2(z). \quad (1)$$

The smaller $\Phi(z)$ the greater the useful head, since the value of h_{T_∞} does not depend on the number of vanes or on \bar{D}_κ . Consequently, expressing the value $\Phi(z)$ as a function of z and \bar{D}_κ we can analyze the influence of z and \bar{D}_κ on the useful head.

The value $f_1(z)$ can be represented as follows:

$$f_1(z) = \frac{h_{T_\infty} - h_r}{h_{T_\infty}} = 1 - \frac{h_r}{h_{T_\infty}} = 1 - \mu, \quad (2)$$

where $\mu = h_r/h_{T_\infty}$ is the coefficient of a decrease in the transmitted energy.

The value Δh_r can be expressed as follows:

$$\Delta h_r = R_x \frac{w_m^2}{G} z, \quad (3)$$

where R_x is the resistance arising with friction in the vane channels; w_m^2 is the mean relative velocity taking into account restriction between sections 1-1 and 2-2 of the impeller; G is the weight flow of the gas.

On the basis of Kearton's experimental data [7], let us express the coefficient μ for wheels with a single-stage cascade according to Ekkert's formula [4]:

$$\mu = \frac{1}{1.5 + 1.1 \frac{\beta_{22}}{90^\circ} + \frac{1}{2z \left(1 - \frac{D_1}{D_2}\right)}}. \quad (4)$$

The expediency of using Formula (4) has been confirmed by our experimental data.

Determination of the function $f_2(z)$ is a more complex problem due to the lack of sufficient experimental data for finding the resistance R_x . To approximately determine the resistance occurring with turbulent gas flow in the vane channels of an annular cascade, let us use, by analogy, the familiar relationship from the theory of fluid flow in channels of arbitrary cross section:

$$R_x = \lambda \frac{1}{2} \rho_m w_m^2 S, \quad (5)$$

where λ is the resistance coefficient; ρ_m is the mean density of the gas in the channel;

$$S = 2(a_m + b_m)l = \frac{\pi D_m \sin \beta_{gm} - \delta z + b_m z}{z} \cdot \frac{D_2 - D_1}{\sin \beta_{gm}};$$

$a_m = \pi D_m / z \sin \beta_{gm} - \delta$ is the width of the vane channel; δ is the vane thickness; and $l = (D_2 - D_1) / 2 \sin \beta_{gm}$ is the arbitrary length of the channel.

The values of the parameters with the subscript m were defined as the arithmetic mean between sections 1-1 and 2-2.

The resistance coefficient λ , according to recommendations by Balje [8], can be calculated from the Blasius formula

$$\lambda = \frac{1}{4} \cdot \frac{0.316}{\sqrt[4]{\text{Re}}}, \quad (6)$$

where

$$\text{Re} = \frac{w_m d_{gm}}{\nu_m};$$

$$d_{gm} = \frac{2a_m b_m}{a_m + b_m};$$

ν_m is the coefficient of kinematic viscosity.

For wheels with a single-stage cascade, using Eqs. (1)-(6) we

get, after transformations,

$$\Phi(z) = 1 - \frac{1}{1 + \frac{1.5 + 1.1 \left(\frac{\beta_{g_2}}{90^\circ} \right)}{2z \left(1 - \frac{D_1}{D_2} \right)}} - \frac{\gamma_m (w_1 + w_2)^2}{64 G u_2^2} \times \quad (7)$$

$$\times \frac{0.316 (D_2 - D_1)}{1 - \varphi_p \cot \beta_{g_1}} \left(\frac{\pi D_m \sin \beta_{g_m}}{\pi D_m \sin \beta_{g_m} - \delta z} \right)^2 \cdot \frac{\pi D_m \sin \beta_{g_m} - \delta z + b_m z}{\sin \beta_{g_m} \sqrt{\frac{w_1 + w_2}{v_m} \cdot \frac{\pi D_m \sin \beta_{g_m} b_m}{\pi D_m \sin \beta_{g_m} - \delta z + b_m z}}}$$

To determine $\Phi(z)$ for wheels with a two-stage cascade we can use Eq. (7), leaving $f_1(z)$ unchanged* and representing friction and vorticity losses of the entire wheel as the sum of the losses in the two stages

$$f_2(z) = f_2(z_1) + f_2(z_2).$$

Figure 2 shows the graphic solution of Eq. (7) for the investigated type of wheels with single- and two-stage cascades. For wheels with a single-stage cascade the optimum number of vanes, with respect to useful head, is within the range $z_{opt} h = 16-23$. Analysis of the curves shows that with increasing \underline{z} , the optimum wheel with a two-stage cascade is obtained for high \bar{D}_κ . From the standpoint of obtaining minimum losses in useful head it is expedient to use wheels with a two-stage cascade beginning with $z > 18-20$.

We should mention the restricted sphere of application of Eq. (7) because of the approximateness of Eq. (6) which defines the value of the resistance coefficient λ without taking into account the presence and development of breakaway zones in the rotating vane channels of

* The experimental data obtained verify the expediency of using Ekkert's equation [4] to calculate the influence of a finite number of vanes of wheels with a two-stage cascade, assuming $z = z_2$.

the wheel, and also without taking into account the effect of the rotation and curvilinearity of the channels. For wheels with $z_2 = z_1$ the expediency of using (7) is limited to the region in which local diffusivity and the exposure angles of the channels are within tolerable limits and, consequently, the presence of developed breakaway zones is not expected, i.e., a region with a sufficiently large number of vanes. Below we give an analysis which makes it possible to establish z for which the level of local diffusivity will be minimal. For wheels with $z_2 = 2z_1$ the restrictions on the equation for determining λ are made more severe by the fact that with very high \bar{D}_κ very short vanes disrupt normal gas flow in the channels of the second stand. In addition, in the region of very large \bar{D}_κ it is hardly possible to reliably determine the coefficient μ from known theoretical and empirical relationships.

It can be assumed that the nature of the dependences $\eta_{a\partial}^* = f(\varphi_{p_0})$ and $\psi^* = f(\varphi_{p_0})$ will be substantially influenced by the breakaway zones which develop in the channels of a centrifugal wheel; the presence and scale of these zones, in turn, depend mainly on the value of local diffusivity. The value of maximum local diffusivity can be estimated by the relation $w_{loc\ max}/w_2$. Considering that the relative velocity w_2 for a single series of wheels with $u_2 = \text{const}$ changes insignificantly, the maximum local diffusivity and, consequently, the degree of development of breakaway zones can be estimated by the value $w_{loc\ max}$ or $M_{loc\ max}$. Such an approach to the study of the influence of breakaway zones on the operational efficiency of a centrifugal wheel considerably simplifies the theoretical analysis, making it possible to simultaneously obtain a value for the maximum local Mach numbers which characterize the operation of the cascade.

There exist various theoretical methods for calculating the local relative velocity in the radial plane of a wheel with a finite number of vanes. However, most of these methods are quite unwieldy and when making calculations they require use of the method of successive approximations. A number of authors [1, 2] have proposed for this purpose a reasonably simple approximate analytical dependence which establishes the connection between the local relative velocity and the coordinates of the examined point. Considering that maximum local relative velocity is attained on the nonacting surface of the vane, the proposed equation for wheels with $\beta_{g_2} < 90^\circ$ is written as follows:

$$w_{np}^r = w_{av}^r \left(1 - \frac{a}{2R_1} \right) + \omega a, \quad (8)$$

where w_{av}^r is the average relative velocity in the investigated section, taking into account restriction and bend of the flow to an angle β_g ; a is the width of the channel in the radial plane; R_1 is the radius of curvature of the vane; and ω is the angular speed of rotation of the wheel.

Equation (8) is applicable for determination of the local relative velocity only in regimes of maximum airfoil cascade flow. Otherwise, due to a change in shape of the flow lines, there is a considerable change in their equidistance from the center line of the vane.

Bearing in mind that

$$w_{av}^r = \frac{G}{\sqrt{F^*}}, \quad \frac{G}{\gamma} = c_z \cdot \frac{\pi}{4} (D_n^2 - D_0^2) \frac{\gamma_0}{\gamma},$$

and using the expression for the Mach number and Eq. (8), we get, finally,

$$\frac{M_{np}^r}{M_{c_0}} = \frac{D_n^2 - D_0^2}{4} \sqrt{\frac{T_0}{T_{np}}} \left\{ \frac{\pi}{\pi D \sin \beta_g - \delta z} \cdot \frac{\gamma_0}{\delta \gamma} \left[1 - \frac{\pi D}{2R_1 z} \sin \beta_g + \frac{\delta}{2R_1} \right] + 8 \frac{\pi D \sin \beta_g - \delta z}{(D_n^2 - D_0^2) D_x^2 \varphi_{p_0}} \right\}. \quad (9)$$

A graphic solution of Eq. (9) for the investigated wheels is shown in Fig. 3. An analysis of the curves in this figure shows that for wheels with $z_2 = z_1$ the optimum number of vanes, from the standpoint of the minimum Mach level or minimum local diffusivity, is within the range $z_{opt} M = 11-13$. For wheels with $z_2 = 2z_1$, with increasing z the minimum level of the development of local diffusivity at the second stage is observed for larger \bar{D}_κ . For any z the maximum value of M_{wnp}'' / M_{cz0} occurs when $\bar{D}_\kappa = 0.527$, i.e., at the inlet to the first stage of the cascade.

In two-stage cascades of the investigated type, to obtain minimum M numbers in the first stage we must select $z_1 = 10-14$, while for minimum M numbers in the second stage we must assume $\bar{D}_\kappa = 0.7-0.8$.

Taking into account the assumptions used to derive Eq. (9), it is to be expected that the absolute values of M_{wnp}'' / M_{cz0} are approximate. However, use of Eq. (9) makes it possible to quite simply estimate the region of the origin of the intense development of break-away zones in vane channels as a function of the geometric relationships of the wheel and the flow parameters.

To determine the influence of the number and length of the vanes on the hydraulic efficiency of a wheel we can use the functions $f_1(z)$ and $f_2(z)$ obtained previously:

$$\begin{aligned} \eta_{gk} &= \frac{h_T - \Delta h_r}{h_T} = 1 - \frac{\Delta h_r}{h_T} = \\ &= 1 - \frac{f_2(z)}{1 - f_1(z)}. \end{aligned} \quad (10)$$

The graphic solution of Eq. (10) is shown in Fig. 3. Analysis of the curves shows that with increasing \bar{D}_κ , when $z = \text{const}$, the hydraulic efficiency of the wheel increases. For the same number of vanes z_2 the efficiency of a wheel with a single-stage cascade is less than that of a wheel with a two-stage cascade. The absence of

a maximum on the $\eta_{g\kappa}$ curves is explained by the above-mentioned restrictions of Eq. (6) which does not take into account the presence of developed breakaway zones in vane channels for wheels with relative sparse cascades with a large channel exposure angle. Using previously obtained data on the influence of \underline{z} and \bar{D}_κ on the value of local diffusivity and, consequently, the level of development of breakaway zones, we can approximately limit the sphere of applicability of Eq. (10) by the curve M-M. To the left of line M-M Eq. (10) should yield a qualitatively incorrect result.

Using simple physical concepts it is easy to show that for increased width of the acting zone of the wheel characteristic it is necessary to decrease restriction of the flow at the inlet [9]. This assumption has been confirmed by experimental data obtained. Consequently, the curve M-M and Eq. (9) determine the optimum number of vanes from the standpoint of attaining the maximum width of the acting zone of the wheel characteristic for a reasonably high efficiency level.

It should be mentioned that the proposed equations (7), (9), and (10) are sufficiently general and can be used to determine the influence on the useful head, the level of local diffusivity, and the hydraulic efficiency of not only \underline{z} and \bar{D}_κ but also of other geometric relationships of the wheel and the flow parameters.

Thus, on the basis of this theoretical analysis we can assume that wheels with two-stage cascades can have advantages over wheels with single-stage cascades with respect to efficiency, head, and width of the acting zone of the characteristic.

2. Experimental Study

The experimental part of the work was done on the ETsK-1 test stand at the Laboratory of Compressor Machines of M. I. Kalinin Leningrad polytechnic University [10]. The diagram of the blading of the stand and the control sections for measuring the flow parameters is shown on p. 16. The wheels were tested for constant peripheral velocity $u_2 = 214.5$ m/sec. In all, 25 shrouded wheels with fully milled vanes were tested ($\beta_{g_2} = 49^\circ$). Of these, 8 had single-stage and 17 had two-stage cascades. The basic geometric parameters of the wheels are shown in Fig. 1 and given in Table 1. In Table 1, the crosses designate wheels tested on the ETsK-1 stand, while the terms "starting" and "derived" cascades indicate, respectively, single-stage cascades with $z = z_2$ and $z = z_1$.

The experimental data were measured and processed according to the Leningrad Polytechnic Institute method [6, 9, 11] using small pneumometric devices developed at LPI [12, 13, 14, 15], and also other measurement and recording apparatus [6, 10-16].

As criteria for estimating the efficiency of the wheels we used parameters examined in detail in previous papers [9, 11]. In addition to the parameters derived in these works, in the present investigation we used the following:

$$M_{\text{max}}^* = \frac{w_k^*}{\sqrt{\gamma g R T_k}} \quad (11)$$

where

$$w_k^* = \frac{c_{rk}}{\sin \beta_{gk}} = \frac{G}{\gamma_k \pi D_k b_k \tau_k \sin \beta_{gk}} \quad (12)$$

τ_k is the coefficient of flow restriction at the outlet from the first stage of the cascade or at the inlet to the second stage, determined from $z = z_1(\tau_{kI})$ or $z = z_2(\tau_{kII})$.

The values of T_{κ} and γ_{κ} were determined approximately, on the basis of the assumption of a linear law of change in temperature and density of the gas between sections 1-1 and 3-3, and the presence of the equalities $T_0 \approx T_1 \approx T_1''$ and $\gamma_0 \approx \gamma_1$.

Analysis of the individual characteristics of the wheels has made it possible to make the following remarks (Fig. 4):

1. The general nature of the individual characteristics of wheels with $z_2 = 2z_1$ does not differ from the corresponding characteristics for $z_2 = z_1$ [9, 11].

2. The nature of the curves $\eta_{ad}^* = f(\varphi_{p_0})$ and $\psi^* = f(\varphi_{p_0})$ is determined by the number of vanes in the starting single-stage cascade $z = z_2$ and the relative diameter \bar{D}_{κ} . With an increase in \bar{D}_{κ} for the given series of wheels, the curve η_{ad}^* becomes more inclined. A similar phenomenon is noted with decreasing z for $\bar{D}_{\kappa} = \text{const}$.

Such a result is completely regular. An increase in \bar{D}_{κ} decreases the total working surface of the vanes and restriction at the inlet and leads (when $\bar{D}_{\kappa} = 1$) to a decrease in the total number of vanes by a factor of two. Therefore an increase in \bar{D}_{κ} and a decrease in z of the starting cascade should have a qualitative influence on the characteristic of the wheel. This inter-dependence of \bar{D}_{κ} and z is evident for other wheel characteristics as well.

3. For all the studied wheels $\eta_{ad}^* \max$ is within the region $i_1 = 0-10^\circ$, while ψ_{\max}^* is within the region $i_1 = 15-24^\circ$.

4. The number M_{w_1} and particularly the numbers M_{w_1}'' and $M_{w\kappa}''$ increase with increasing flow rate. In this case the relation between the values $M_{w\kappa}''$ and M_{w_1}'' depends on the value \bar{D}_{κ} . As a rule, $M_{w\kappa}'' < M_{w_1}''$; however, with large z and very small undercuts we have the inequality $M_{w\kappa}'' > M_{w_1}''$.

Analysis of the comparative characteristics of wheels with two-stage cascades makes it possible to make the following remarks (Fig. 5):

1. With increasing \bar{D}_κ and decreasing z the zone of economic and stable wheel operation increases.

2. The value of η_{a0}^* depends on \bar{D}_κ and z . The dependence $\eta_{a0}^* \max = f(\bar{D}_\kappa)$ has an extremal value. For all series of wheels, with increasing \bar{D}_κ there is first an increase in the efficiency to its maximum value, then it decreases, and finally, when $\bar{D}_\kappa > 0.8-0.9$, it again increases somewhat. The nature of these curves can be explained as follows.

Transition to a two-stage cascade due to undercutting at the inlet of the vanes results in decreased restriction of the flow (an increase in τ) and an increase in the channel exposure angle ν of the first stage compared with the same sections of the starting cascade. For the first stage of vanes, with a further increase in D_κ the values of τ_1 and ν_1 remain constant, τ_κ increases, while ν_κ decreases slightly. For rather large z , there will be, at the starting cascade, great restriction and a small channel exposure angle at the inlet. A small τ_{1st} (large M_{w1st}'') will have a negative influence on the operation of the cascade. The influence of small ν_{1st} will, however, be insignificant. By undercutting the vane of such a starting cascade we first decrease the negative influence of great flow restriction. The influence of undercutting the vanes, however, on the increase of the angle ν_1 is less clearly expressed. Therefore, when undercutting the vanes in the starting cascade with high ν we can likely expect increased efficiency. A further increase in \bar{D}_κ will involve a decrease in flow restriction and flow surface friction against the vanes. This leads simultaneously to an increased load on the vane apparatus and,

consequently, to increased local Mach numbers and local diffusivity on the airfoil, and also to an increase in the part of the channel having a large exposure angle. Because of these factors, beginning at a certain \bar{D}_κ there is a reduction in efficiency.

The negative influence of these factors for large undercuts, for the given wheels with $\bar{D}_\kappa > 0.8-0.9$, is intensified by the fact that the short vanes of the second stage of the cascade cease to operate as aerodynamic airfoils and are essentially additional resistance. Therefore, with further undercutting of the vanes, right up to complete shearing of the vanes, there is a certain increase in efficiency.

These concepts make it possible to assume that if the starting cascade has small \underline{z} , i.e., large $\tau_{1\text{ st}}$ (small $M_{w_{1\text{ st}}}''$) and large angle $\nu_{1\text{ st}}$, undercutting of the vanes may not increase the efficiency but, conversely, lower it. In this case a positive influence of the two-stage cascade on wheel operation can be attained by installing additional short vanes at the outlet. This decreases the local diffusivity of the channel at the exit and evidently decreases the intensity of the turbulent region on the nonacting surface of the vanes. This analysis shows that the larger the \underline{z} of the starting cascade, the larger will be the values of \bar{D}_κ for which the optimum operating regimes of a two-stage cascade will be attained. Experimental data have confirmed this conclusion.

3. The head coefficient ψ_{opt}^* is a function of \bar{D}_κ and \underline{z} . With a relatively small number of vanes ($z = 16-24$) for the starting cascade an increase in \bar{D}_κ causes a decrease in ψ_{opt}^* . With increasing \underline{z} the region of decreasing ψ_{opt}^* decreases.

The decrease in ψ^* with small \underline{z} , particularly for slight undercuts, is evidently associated with a sharp (two-fold) increase in the

angle ν_1 in the cascade of the first stage (compared with the starting cascade), while the other factors are weakly expressed.* We should note that with relatively small \underline{z} the conditions of flow inlet to the cascade influence the direction of the outlet velocity and, consequently, the head.

For large \underline{z} , when the angles ν_1 are small and their influence is not substantial, undercutting of the vanes, which lowers the restriction of the flow and decreases energy lost to friction of the gas against the vanes, can cause an increase in the load on the vane apparatus and the diffusivity of the channels of the first stage. In connection with the above, the nature of the change in ψ_{opt}^* for undercutting of the vanes in a two-stage cascade will depend on the relation between these coefficients at the starting and derived cascades.

4. The values of $\varphi_{p_{0opt}}$ and $\varphi_{p_{0cr}}$ depend on \bar{D}_κ as well as on \underline{z} . With increasing \bar{D}_κ for all wheel series there is an increase in $\varphi_{p_{0opt}}$ and a decrease in $\varphi_{p_{0cr}}$. The greatest change in $\varphi_{p_{0opt}}$ and $\varphi_{p_{0cr}}$ is observed in the zone $\bar{D}_\kappa \approx 0.55-0.62$. For large \bar{D}_κ the values of $\varphi_{p_{0opt}}$ and $\varphi_{p_{0cr}}$ remain practically constant and only when $\bar{D}_\kappa > 0.85-0.9$ and for small \underline{z} is there again a certain decrease in $\varphi_{p_{0cr}}$ for large \bar{D}_κ , while for large \underline{z} (series 24/12) there is no decrease whatsoever.

The shift in the maxima of η_{ad}^* and ψ^* vs. \bar{D}_κ and \underline{z} can be explained by the influence of the change in the value of τ_1 and τ_κ on the ratio between M_{w_1}'' and M_{w_1cr}'' , and M_{w_κ}'' and $M_{w_\kappa cr}''$.

The abrupt shift of the maximum efficiency toward higher flow rates when $\bar{D}_\kappa \approx 0.58-62$ can evidently be explained by the sharply

* We should mention that the question of the influence of the angles ν on operation of the cascade is a complex problem, one that has been little studied. Special studies are required to solve it.

decreased restriction of flow at the inlet and, consequently, by the sharp decrease in M''_{w_1} compared with M''_{w_1st} .

An increase in \bar{D}_κ , in final analysis, decreases flow restriction in a two-stage cascade and therefore it in principle should lower the value of φ_{p_0cr} . The greatest decrease in φ_{p_0cr} for $\bar{D}_\kappa \approx 0.58-0.62$ is evidently explained in the same way as the increase in φ_{p_0opt} in this region. The decrease in φ_{p_0cr} for $\bar{D}_\kappa > 0.85-0.9$ can be associated with the fact that further undercutting of the vanes, eliminating the inefficient airfoils of the second stage of the cascade, results in improved flow aerodynamics and, consequently, an increase in the $M''_{w_1} \approx M''_{w_1cr}$ numbers in the cascade channels. Therefore retention of the inequality $M''_{w_1} \approx M''_{w_1cr}$ is now possible for larger i_1 (smaller φ_{p_0}). With increasing z and, consequently, decreasing load on the vanes and angle ν , the influence of greatly shortened vanes on the flow aerodynamics decreases. Therefore there is less of a decrease in φ_{p_0cr} in the region $\bar{D}_\kappa > 0.85-0.9$, while for the series of wheels beginning with 24/12 there is none whatsoever.

Analysis of the curves $k_y = f(\bar{D}_\kappa)$ shows that the width of the acting zone of the characteristic depends on \bar{D}_κ and on z . In the region $\bar{D}_\kappa \approx 0.58-0.62$ there is a sharp expansion of the acting zone of the wheel characteristic. A further increase in \bar{D}_κ does not result in a substantial change in k_y , and only when $\bar{D}_\kappa > 0.85-0.9$ for small z is there again observed an increase in k_y . There is less expansion of the acting zone of the characteristic in this range of changes of \bar{D}_κ with increasing z , while for the series of wheels beginning with 24/12 there is no expansion. The nature of the change in k_y vs. \bar{D}_κ and z is determined by the corresponding shift in the maximum efficiency and head coefficient.

5. The relative flow nonuniformity with respect to energy (the coefficients $k_{h\ a\delta}^*$ and $k_{h\ 1}$) does not depend on \bar{D}_κ and \underline{z} .

The relative flow nonuniformity with respect to angle and flow rate (the coefficients k_α and k_G) depends on \bar{D}_κ . With an increase in \bar{D}_κ to 0.76-0.8 the coefficients k_α and k_G remain practically constant. A further increase in \bar{D}_κ leads to an increase in k_α and k_G . This latter can evidently be explained by the above-mentioned negative influence of the greatly shortened vanes of the second stage of the cascade. Removal of these vanes again decreases k_α and k_G . As is to be expected, the surge on the curves of k_α and k_G for $\bar{D}_\kappa > 0.76-0.8$ corresponds to a certain decrease efficiency in this zone.

The shape of the curve of the absolute flow nonuniformity with respect to the angle $\Delta\alpha = f(\bar{D}_\kappa)$ is basically identical with that of the curve $k_\alpha = f(\bar{D}_\kappa)$, and can be explained by the same reasons.

6. The numbers M_{w_1} and M_{w_1}'' depend on \underline{z} and also \bar{D}_κ for $\eta_{a\delta}^* \max$. The numbers M_{w_1} and M_{w_1}'' , with increasing \bar{D}_κ , increase somewhat. This is due to the fact that an increase in \bar{D}_κ results in an increase in $\varphi_{p_0 \text{opt}}$ and, consequently, in w_1 and w_1'' and, respectively, M_{w_1} and M_{w_1}'' . With increasing \underline{z} $\varphi_{p_0 \text{opt}}$ decreases, which lowers M_{w_1} . The value of M_{w_1}'' with increased \underline{z} is greatly influence by the increased flow restriction which increases w_1'' , and therefore M_{w_1}'' increases.

3. Comparison of the Results of a Theoretical Analysis with Experimental Investigations

Wheels with a Single-Stage Cascade. The proposed equation (7) for estimating the influence of various geometric criteria of a wheel and the flow parameters on the value of the useful head can be used also to determine the optimum number of vanes. The graphic solution

of this equation, given in Fig. 2, shows that the optimum number of vanes from the point of view of attaining maximum useful heads for the investigated wheels is in the region $z_{\text{opt } h} = 16-23$. From experimental studies $z_{\text{opt } h} = 14-20$. Thus, the experimental data obtained confirm the expediency of using theoretical dependence (7).

The possibility of using Eq. (9) for determining the optimum number of vanes from the standpoint of achieving the maximum width of the acting zone of the wheel characteristic with a sufficiently high efficiency has been confirmed by experimental data obtained. For the investigated wheels $z_{\text{opt } M} = 10-14$ vanes. According to experimental results $z_{\text{opt } M} = 11-13$. In this case, compared with a wheel with $z_2 = z_1 = 16$ k_y increases 2- to 3-fold, while the efficiency only decreases 1.5-2.0%.

Wheels with a Two-Stage Cascade. The proposed equation (7), from a qualitative standpoint, correctly evaluates the influence of z and \bar{D}_κ on the losses of useful head in a wheel with a two-stage cascade. Analysis of this equation shows that with increasing \bar{D}_κ the optimum number of vanes $z_{\text{opt } h}$ increases. From the point of view of achieving minimum losses of useful head, use of the two-stage cascade is justified only when $z_2 \geq 18-20$. This agrees with experimental data obtained, in accordance with which $z_{2\text{opt } h} > 24$.

The use of Eq. (7) to calculate $z_{\text{opt } h}$ in the region of large \bar{D}_κ leads to quantitatively incorrect results because of the mentioned restrictions on dependence (6) due to the negative influence of the greatly shortened vanes of the second stage.

Comparison of theoretical and experimental data makes it possible to confirm that Eq. (9) can be used to determine the optimum values of z and \bar{D}_κ for wheels with a two-stage cascade from the point of view

of attaining maximum width of the acting zone of the characteristic with reasonably high efficiency. The theoretical and experimental curves in the region $\bar{D}_\kappa < 0.8$, shown in Fig. 6, practically coincide.

Shrouded wheels having a single-stage cascade of normally backward bent vanes with $z_2 = z_1 = 16-24$ are widely used in stationary centrifugal compressors. The conversion from single-stage cascades of such wheels to two-stage cascades with $z_2 = 2z_1$ makes it possible to increase the efficiency and expand the acting zone of the wheel characteristic (Fig. 6). True, with relatively small z (in our case $z_2 = 16$ and 20), this involves a certain reduction in $\eta_{ad}^* \max$ and k_y , as well as with respect to ψ^* .

The relative increase (positive or negative) in the values of $\eta_{ad}^* \max$, k_y , and ψ_{opt}^* for optimum two-stage cascades of each series, compared with their starting single-stage cascades and with an optimum single-stage cascade having $z = 16$,* is shown in Table 2.

Our experimental study has made it possible to make a qualitative and quantitative estimate of the influence of z and \bar{D}_κ on the operating efficiency of a wheel with a two-stage cascade. The quantitative data obtained, strictly speaking, are valid only for specific wheel and flow parameters, i.e., for specific β_{g1} , $\beta_{g\kappa}$, β_{g2} , D_1/D_2 , δ/D_2 , shape of the leading edge of the vanes, etc. A change in these parameters compared with those used in the experiments might have the result that the influence of z and \bar{D}_κ would change quantitatively, to a certain extent. It should be noted, however, that our study was made for wheels constructed according to generally accepted recommendations

* Investigations of the LPI [8] showed that the optimum single-stage cascade, from the standpoint of maximum efficiency and head for the given wheel geometry, is obtained when $z_2 = z_1 = 16$.

for typical wheels of stationary low-output centrifugal compressors.

Use of the obtained theoretical dependences makes possible a qualitative and quantitative analysis of cascades for various geometric dimensions of a wheel and distinct flow parameters.

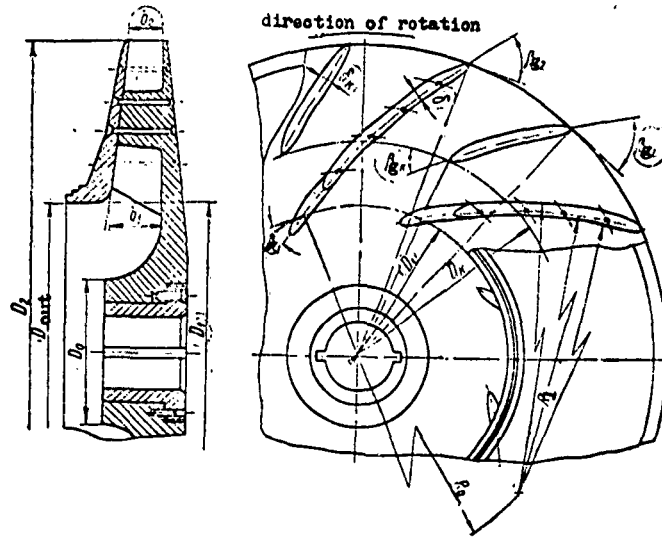


Fig. 1. Diagram of the investigated wheels.

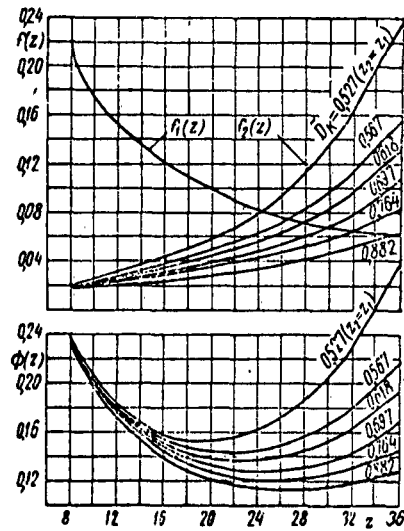


Fig. 2. Determination of $z_{opt h}$ of wheels with single- and two-stage cascades.

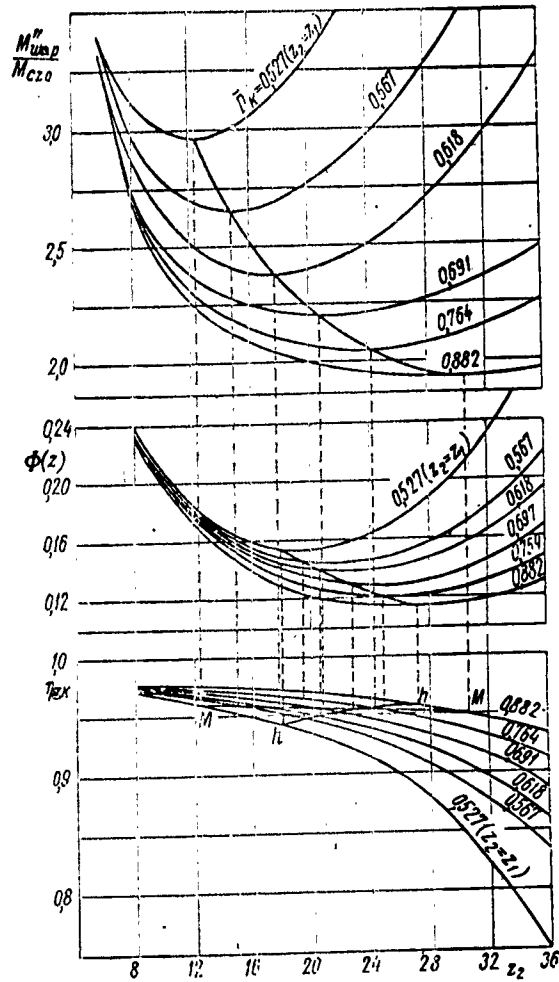


Fig. 3. The effect of z and \bar{D}_k on the level of local M numbers, losses in useful head, and hydraulic efficiency.

TABLE 1
Geometric Parameters of the Investigated Wheels

Parameters		Relative diameter $\bar{D}_k = D_k/D_0$						
		Starting cascade	Two-stage cascades					Derived cascade
			0,827	0,867	0,818	0,801	0,764	
Variable	D_k (mm)	145	156	170	190	210	242,5	275
geometric	β_k (deg)	33°42'	37°9'	40°37'	43°37'	45°58'	47°56'	49°
parameters	b_k (mm)	28	26,9	25,5	23,5	21,5	18,25	15
z_2/z_1	16/8	+	-	+	+	+	+	+
	20/10	+	+	+	+	+	+	+
	24/12	+	-	+	+	+	+	+
	28/14	+	-	-	-	+	+	+
	32/16	-	-	-	-	+	+	+

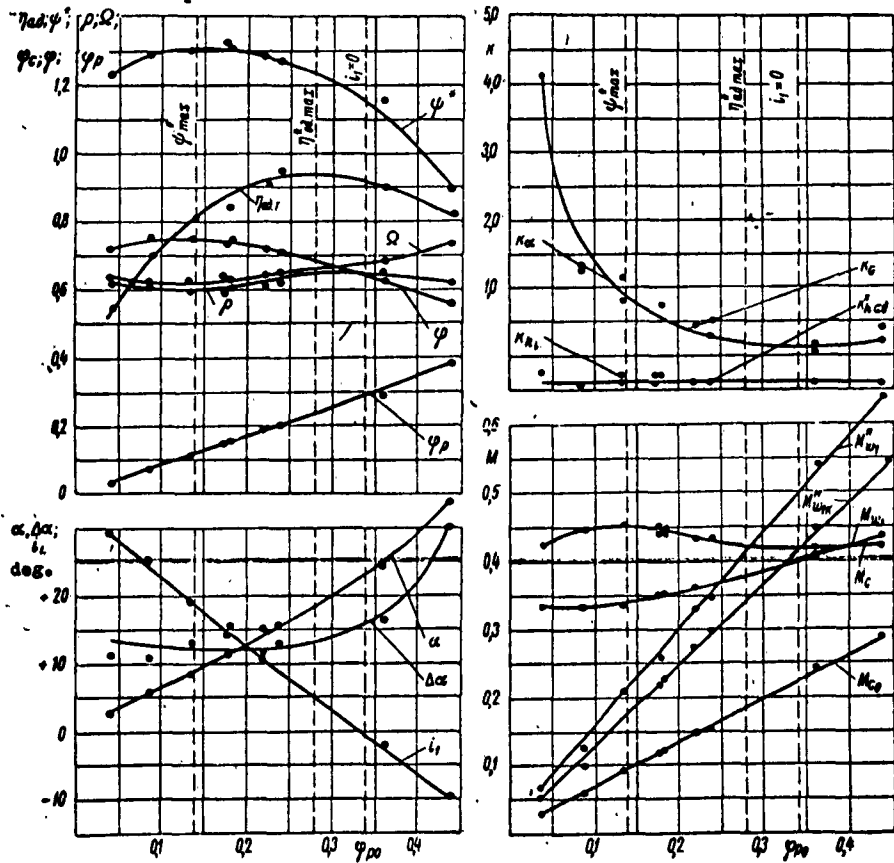


Fig. 4. Individual characteristics of wheels of the series 20/10, $\bar{D}_k = 0.618$.

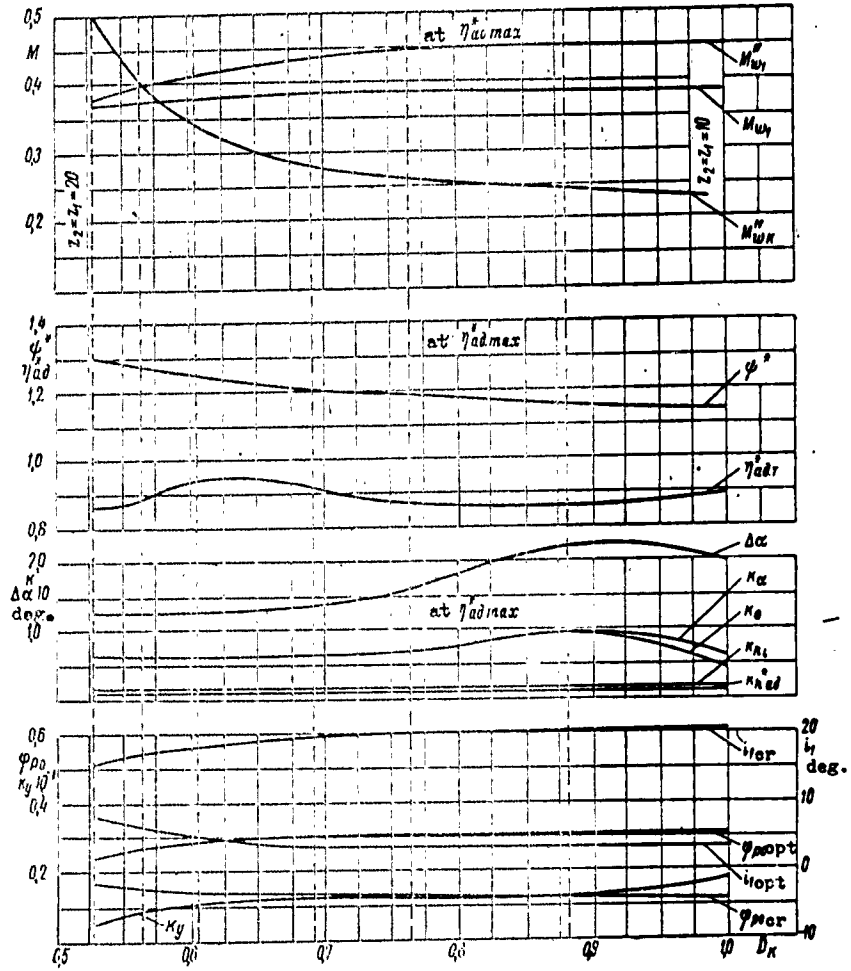


Fig. 5. Comparative characteristics of wheels of the series 20/10 ($\Delta\alpha_{\max} \approx 22^\circ$).

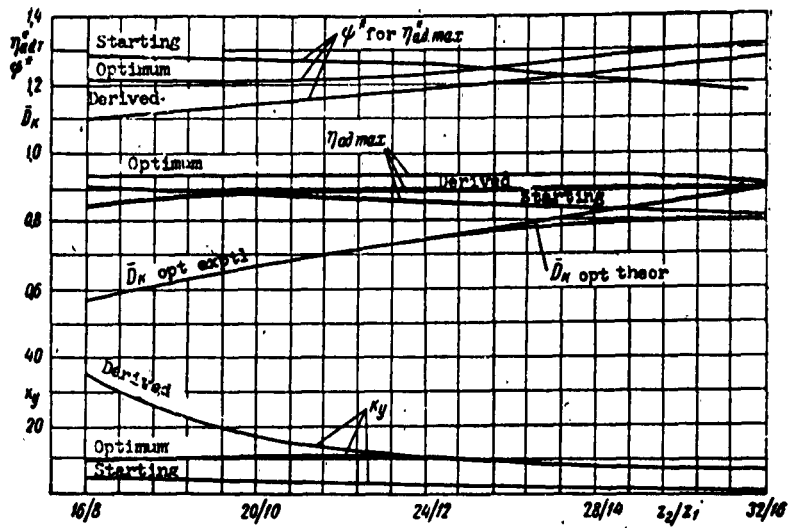


Fig. 6. Comparative characteristic of wheels with starting and derived single-stage, and optimum two-stage, cascades.

TABLE 2

Comparison of Wheels with Single- and Two-Stage Cascades

z_2/z_1	B_{kopt}	Comparison with starting single-stage cascade of the given series		Comparison with optimum single-stage cascade $z_2 = z_1 = 16$	
		$\frac{\Delta \eta_{ad}}{\eta_{ad}} \%$	$\frac{\Delta \psi}{\psi} \%$	$\frac{\Delta \eta_{ad}}{\eta_{ad}} \%$	$\frac{\Delta \psi}{\psi} \%$
16,8	0,59	+4	-3,2	+4	-3,2
20/10	0,65	+6	-3,9	+4	-2,4
24/12	0,75	+9	-4	+3,5	-4,7
28/14	0,79	+11	+6,5	+4	+2,3
32/16	0,8	-	-	+1,0	+4

REFERENCES

1. Yu. S. Podobuyev and K. P. Seleznev. Teoriya i raschet osevykh tsentrobezhnykh kompressorov, Mashgiz, 1957.
2. V. F. Ris. Tsentrobezhnyye kompressornyye mashiny, Mashgiz, 1951.
3. V. F. Ris. Iz opyta proyektirovaniya kompressornykh mashin na NZL, Trudy NZL, vol. I, TsBNTI, 1957.
4. B. Ekkert. Osevyye i tsentrobezhnyye kompressory, Mashgiz, 1959.
5. V. M. Kulakov. O chisle lopatok v kolese turbokompressora, Trudy MVTU im. Baumana, 1958, No. 75.
6. F. S. Rekstin. Vliyaniye odnositel'nogo shaga krugovoy reshetki koleasa tsentrobezhnogo kompressora na effektivnost' koleasa, Nauchno-tekhnicheskii informatsionnyy byulleten', LPI, 1959, No. 12.
7. W. Kearton. The influence of the number of impeller blades on the pressure generated in a centrifugal compressor and on its general performance, Proc. Inst. Mech. Eng., 1933, vol. 124.
8. O. E. Balje. Contribution to the problem of designing radial turbomachines, Trans. A. S. M. E., 1952, May.
9. S. A. Anisimov, et al. Vliyaniye chisla lopatok na effektivnost' tsentrobezhnogo koleasa s odnoyarusnoy reshetkoy. See p. 20 of this collection.
10. F. S. Rekstin. Stend ETsK-1 laboratorii kompressornykh mashin LPI im. M. I. Kalinina, Nauchno-tekhnicheskii informatsionnyy byulleten', LPI, 1959, No. 6.
11. S. A. Anisimov. Issledovaniye raboty koleasa tsentrobezhnogo kompressora. See p. 1 of this collection.
12. S. A. Anisimov, et al. Sravneniye malogabaritnykh trubok polnogo davleniya, Nauchno-tekhnicheskii informatsionnyy byulleten', LPI, 1959, No. 6.
13. Ibid., No. 12.
14. S. A. Anisimov, et al. Nekotoryye rekomendatsii po ispol'sovaniyu uglomerov dlya issledovaniya potoka v protochnoy chasti model'nykh tsentrobezhnykh kompressorov, Nauchno-tekhnicheskii informatsionnyy byulleten', LPI, 1959, No. 12.
15. Yu. B. Galerkin and F. S. Rekstin. Malogabaritnyy nasadok polnogo davleniya s protokom, Nauchno-tekhnicheskii informatsionnyy byulleten', LPI, 1960, No. 6.

16. F. S. Rekstin. Koordinatnik dyla issledovaniya potoka v protochnoy chasti tsentrobezhnogo kompressora, Nauchno-tekhnicheskiy informatsionnyy byulleten', LPI, 1959, No. 6.

CALCULATION OF VARIABLE REGIMES OF CASCADE FLOW

V. A. Zysin

When investigating one-dimensional flow and, in particular, when analyzing variable regimes of operation of a turbine stage, great importance may be attached to the clearness and relative simplicity of the calculation methods used. This is particularly important in the case of supercritical flow regimes.

Here it might be of great help to introduce an i - S diagram with a grid of the dynamic characteristics — lines of constant specific flow rates (Fanno lines) [4, 5]. This would make it possible, e.g., to directly determine the state of the supersonic flow behind the turbine impeller if there is overexpansion relative to the given counterpressure, to detect the possibility of flow choking, and to solve a number of calculation problems.

However, for practical application it is necessary that the diagram be generalized. Here it is desirable that the coordinates of the dimensionless parameters to be determined and the selected scale be most adaptable to the usual methods of turbine design.

In the present article we propose using a generalized diagram, similar in structure to the ordinary i - S diagram, for a calculation

analysis of the variable regimes of turbine cascade operation.

Calculations using this method aim to explain the most general regularities. Therefore, all processes are schematized to the utmost: we use the stream theory, assume that the velocity and flow factors are identical, do not take into account ejection, leakages, etc.

In light of the above, the methods herein proposed are not intended to replace profound gasdynamic calculations which strive to take into account to the fullest possible extent the influence of various factors.

1. The Generalized Dynamic Diagram

Figure 1 shows a generalized dynamic diagram constructed for an ideal gas with an isentropic exponent $k = 1.3$.

The diagram itself and the method for constructing it have been described previously [1]. Therefore, let us limit ourselves to a brief examination of it.

The diagram was constructed for isoenergetic flow with irreversible losses. Consequently,

$$\left. \begin{aligned} i_0 = i + A \frac{c^2}{2g} = \text{const.} \\ ds > 0, \end{aligned} \right\} \quad (1)$$

where i_0 is the stagnation enthalpy, $A = 1/427$ is the thermal equivalent of work, c is the velocity, and s is the entropy.

Along the abscissa is plotted dimensionless entropy:

$$z = \frac{\Delta s}{AR} = \ln \frac{p_0}{(p_0)_{z=0}} = \ln P_0, \quad (2)$$

where p_0 is the stagnation pressure for the given entropy, $(p_0)_{z=0}$ is the stagnation pressure for $z = 0$, p is the dimensional static pressure, $P = p/(p_0)_{z=0}$ is dimensionless pressure, and R is the gas constant.

For convenience in using the diagram the abscissa contains a

uniform scale of dimensionless pressures.

Along the ordinate (from top to bottom) is plotted the dimensionless velocity

$$\lambda = \frac{c}{a^*} = \frac{c}{C\sqrt{T_0}} \quad (3)$$

where $C = \sqrt{2g k/(k+1) R}$ is a constant, a^* is critical velocity, and T_0 is the absolute stagnation temperature.

The diagram contains a grid of dimensionless isobars $P = \text{const}$ and a grid of constant reduced flow rates (dimensionless Fanno lines)

$$\Phi = \frac{c\gamma}{(c\gamma)_{z=0}^*} = \text{const.} \quad (4)$$

Here γ is the specific weight, and $(c\gamma)_{z=0}^*$ is the critical specific flow rate (mass flow rate) at zero entropy.

From the upper left-hand corner of the diagram are drawn flow-lines with constant velocity-loss coefficients ϕ or ψ .

If, parallel to the ordinate, we plot the vertical scales of M , T/T_0 , and the other gasdynamic functions, then when using the diagram it is not necessary to resort to gasdynamic tables.

In addition, on the diagram we could plot grids of the dynamic characteristics which would make it possible to calculate the compression shocks. In Fig. 1, for simplicity, these additional constructions are omitted.

2. A Cascade for Subsonic Velocities

Figure 2 shows, in λ - z coordinates, the process in a turbine cascade for subcritical flow regimes.

When using one of the usual methods for calculating a turbine for a variable regime, the use of a diagram can facilitate determination of the state of the flow behind the cascade, if the parameters of the incoming flow are given.

Actually, knowing the dimensional relative velocity of the incoming flow c and the critical velocity a_c^* , we can determine the corresponding dimensionless velocity $\lambda_c = c/a_c^*$. From this, on the λ - z diagram, we find the point a which corresponds to the state of the flow entering the cascade.

Let us calculate the reduced flow rate on leaving the cascade:

$$\Phi_e = \Phi_a \frac{\sin \alpha}{\sin \alpha_1} \cdot \frac{h}{h_c}, \quad (5)$$

where h is the height of the vanes of the preceding cascade or the height of the guide channel, h_c is the height of the vanes at the exit from the calculated cascade, α is the angle formed by the cascade axis and the vector of the incoming velocity, α_1 is the angle formed by the cascade axis and the exit axis of the vane channel; Φ_a is the reduced flow rate of the incoming flow, and Φ_e is the reduced flow rate on emerging from the cascade.

Having determined from certain concepts the velocity coefficient for the cascade φ , let us find, at the intersection of the lines $\Phi = \text{const}$ and $\varphi, \psi = \text{const}$, the point b which corresponds to the flow state at the exit section. From this we determine directly the dimensionless exit velocity λ_{c_1} , the corresponding dimensionless pressure P_e , and the ideal exit velocity λ_{c_0} .

When using the generalized diagram it is easy to detect certain phenomena which can occur in variable operation regimes.

For example, it may be that the line Φ_e corresponding to the reduced flow rate at the impeller exit (Fig. 3) does not intersect the line φ, ψ . This indicates choking, during which the exit section of the cascade cannot handle the given flow. From the diagram we can immediately determine the maximum flow which the impeller can handle for the given parameters of total stagnation ahead of it. This flow

is determined by the reduced flow ϕ_e , the line of which touches the curve ϕ, ψ , at point m .

3. A Cascade for Supersonic Flow Velocities

Let us examine a cascade consisting of a Laval nozzle. When analyzing the process of expansion in nozzles we should take into account the difference in losses in the convergent and divergent parts of the nozzle. Often we can consider that all losses are concentrated in the divergent part [3]. Then point k on the λ - z diagram (Fig. 4) corresponds to the state of the flow in the sonic throat. Assuming that the flow fills the entire exit section of the nozzle, let us determine the reduced flow in this section

$$\phi_e = f_{\min}/f_e,$$

where f_{\min} is the area of the sonic throat, and f_e is the area of the exit section.

Similarly, let us find the point b which corresponds to the state of the flow in the exit section at the intersection of the lines $\phi = \text{const}$ and $\phi_e = \text{const}$.

If losses in the convergent part cannot be neglected, i.e., the flow factor $\chi < 1$, the reduced flow in the sonic throat

$$\phi_m = \chi.$$

It is appropriate to note that in this case the sonic throat is characterized on the diagram by the point m which has the corresponding dimensionless velocity $\lambda_m = 1$.*

* From the diagram we can immediately see that according to the stream theory the velocity is subsonic in the sonic throat of an actual Laval nozzle.

The throat is defined by the point k' on the intersection of the line $\phi = \text{const}$ (ϕ for the convergent part of the nozzle) with the line $\lambda = 1$.

The reduced flow in the exit section

$$\phi_e = f_{\min}/f_e \chi.$$

The position of the throat (in the divergent part of the nozzle) is determined from the relationship

$$f_{\kappa}/f_{\min} = \phi_m/\phi_{\kappa},$$

where ϕ_{κ} is the reduced flow at the point k' .

Further, there are possible two basic regimes, depending on one of the following conditions:

1) the relative rate of flow into the next cascade is supersonic,
or

2) the relative rate of flow into the next cascade is subsonic.

In the first case we can assume that the static pressure in the axial clearance does not change, and the next cascade is calculated in the usual manner.

If as a result of this calculation it appears that the state of the flow behind the cascade is characterized by a point on the diagram in the region $\lambda < 1$, we should be on the lookout for choking in the given stage.

In the second case, when the rate of flow into the next stage, obtained from the velocity triangle, is subsonic, pressure in the axial clearance in the general case will differ from the pressure in the nozzle exit section, and will depend on the amount of pressure drop in subsequent stages, and on the counterpressure.

If the pressure in the axial clearance p_n is defined in some way or other, the cascade operating in the region of supersonic velocities is calculated as a function of the sign of the inequality

$$p_e \leq p_n.$$

where p_e is the static pressure in the exit section of the cascade.

If $p_e > p_n = p_{n_1}$, there should be divergence in the transverse section. Let point \underline{b} (Fig. 4) define the state of the flow in the nozzle exit section. This section has the corresponding dimensionless pressure p_e and the dimensionless velocity λ_{c_1} (in the case of convergent nozzles point \underline{b} can lie only on the line $\lambda = 1$).

Let us determine the dimensionless pressure in the axial clearance

$$p_{n_1} = p_{n_1}/p_0,$$

where p_0 is the total pressure (static and dynamic) ahead of the nozzles.

The state of the flow behind the transverse section is defined by the point n_1 at the intersection of the isobar P_{n_1} with the line $\phi, \psi = \text{const.}$ The dimensionless velocity $\lambda_{c_1 n_1} > \lambda_{c_1}$ and the reduced flow ϕ_{n_1} correspond to the point n_1 . From the ratio ϕ_{n_1}/ϕ_e we can find the divergence in the transverse section by one of the familiar methods. If we consider that there are no losses in the transverse section, point b_1 on the vertical dropped from point \underline{b} onto the isobar P_{n_1} corresponds to the state of the flow behind the section.

When the pressure in the cascade exit section is lower than that in the axial clearance, strong shock waves are unavoidable.

If we assume that the flow is not separated from the walls at the end of the vane channel, the state behind the exit section is defined by the intersection of the line ϕ_e with the dimensionless

isobar corresponding to the given pressure in the axial gap. Figure 4 shows cases when, depending on the counterpressure, the terminal velocity remains supersonic (the point n_2) or becomes subsonic (the point n_3). Actually, within the nozzle and in the exit stream, there occurs a system of compression shocks accompanied by separation of flow from the walls. Naturally, it is impossible to analyze such phenomena on the basis of a model of one-dimensional flow used in the given calculation method. At present it is most correct to use experimental data.

However, we can state that the calculation method given here gives maximum losses. Actually, if there is flow separation from the walls (or vice versa) on intersection of the shock front in the free stream, the current density increases. Consequently, the new reduced flow Φ_e is greater than the reduced flow Φ_e which corresponds to flow without separation. But now expansion to the given dimensionless pressure p_{n_2} or p_{n_3} is given not by the points n_2 and n_3 , but by the points $n_2^!$ and $n_3^!$ respectively. Figure 4 shows directly that in this case the value of the terminal entropy decreases, while the velocity increases.

4. Calculation of a Cascade for Choking

Above we examined the case when the cascade cannot pass the given flow due to insufficient area of the exit sections.

It has been shown experimentally that often flow choking is caused by the angle of attack at the cascade inlet [2]. Actually, we know that a decrease in current density corresponds to a flow shock into the concave part of the vane, while an increase in current density corresponds to a flow shock into the convex part. In this

latter case there is the danger of flow choking by the leading edges of the cascade.

If the relative velocity of the incoming undisturbed flow has the corresponding reduced flow ϕ_∞ , the reduced rate of flow into the cascade

$$\phi_{in} = \phi_\infty \sin(\beta_1 - \delta) / \sin \beta_1, \quad (6)$$

where δ is the angle of attack, considered positive for a shock into the concave surface; and β_1 is the inlet angle of the vane apparatus.

Obviously, even in the ideal case it is necessary that

$$\phi_{in} < 1.$$

From this condition we can determine the negative angle of attack for which there will be no flow choking on entry into the cascade. Considering the finite thickness of the leading edges and the additional irreversible losses, we should consider that for subsonic velocity of the incoming flow we must assume the probability of choking at $\phi_e > 0.975$, to which correspond (at $k = 1.3$) the values of the dimensionless velocity $\lambda_{in} > 0.85$. In the case of slight overlappings for thick leading edges, choking occurs even earlier.

When the incoming flow is supersonic, the danger of choking exists continually with negative angles of attack.*

It may be that the section limiting the flow is located in the vane channel, if in the latter the cross section is minimum.

The cascade in this case can be preliminarily checked as follows.

We construct a graph on which along the abscissa is plotted the

* For example, experiments conducted at Leningrad Polytechnic Institute and the Central Scientific Research Institute for Boilers and Turbines revealed choking in all cases when the supersonic incoming flow had negative angles of attack [2].

chord of the airfoil \underline{b} , and along the ordinate is plotted the reduced flow, using as unity the critical flow on entry into the cascade ϕ_a^* (Fig. 5).

The critical reduced flow at the cascade exit

$$\phi_b^* = P_c,$$

where: P_c is the dimensionless pressure at point \underline{c} (Fig. 2).

If we assume that there is uniform loss in head along the chord of airfoil \underline{b} , $dz/db = \text{const.}$ The change in critical reduced flow in the vane channel is thus depicted by the straight line A-B (Fig. 5).

On this same graph we can plot the curve of the change in reduced flow in the channel:

$$\phi_n = \phi_a = f_a/f_n,$$

where ϕ_n is the reduced flow in the given section, and f_a is the area of the corresponding section, determined from the drawing.

If the line ϕ_n intersects line A-B which corresponds to the critical flows (segment C'-D' in Fig. 5), we should suspect that the vane channel will not be able to handle the given flow.

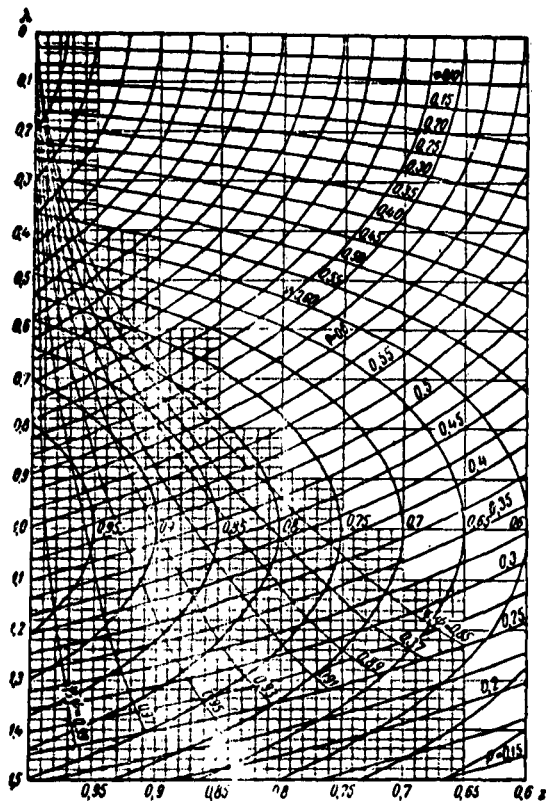


Fig. 1. Generalized diagram for velocity ($\lambda = c/a^+$) minus entropy ($z = \Delta s/AR$). Abscissa — scale of dimensionless pressure.

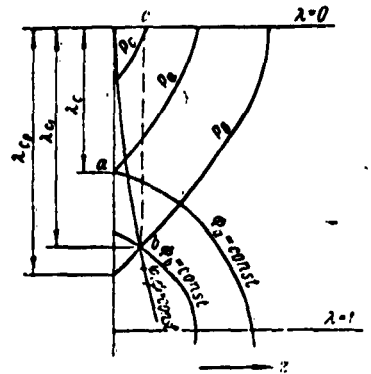


Fig. 2. Representation of the process in an airfoil cascade on a λ - z diagram for $\lambda < 1$.

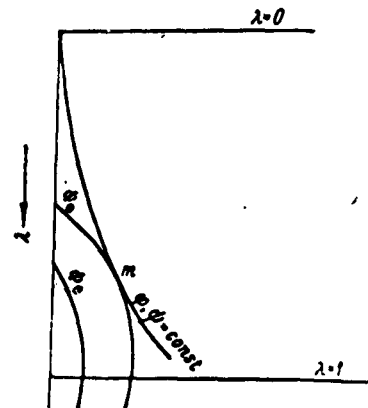


Fig. 3. Case in which the exit section will not handle the given flow.

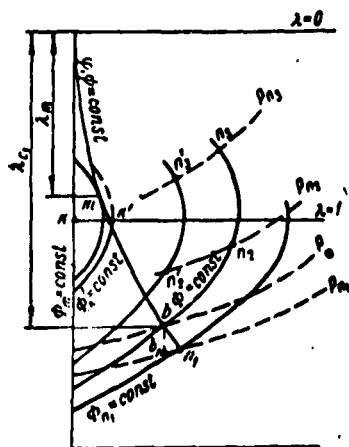


Fig. 4. The process in Laval nozzles.

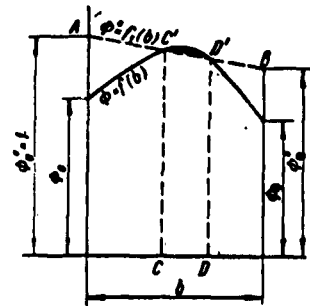


Fig. 5. Checking the vane channel for choking.

REFERENCES

1. V. A. Zysin. Grafoanaliticheskiy metod rascheta odnomernykh potokov szhimayemoy zhidkosti. Trudy LIP, No. 2, 1954.
2. V. A. Zysin, et al. Teploenergetika, No. 2, 1955.
3. I. I. Kirillov, and S. A. Kantor. Teoriya i konstruktsiya parovykh turbin, Mashgiz, 1947.
4. A. Stodola. Dampf und Gasturbinen, VI Auflage, 1924.
5. J. Kestin. J. M. E. Proc., Vol. 159, 1948.

DISTRIBUTION LIST

DEPARTMENT OF DEFENSE	Nr. Copies	MAJOR AIR COMMANDS	Nr. Copies
		AFSC	
		SCFDD	1
		ASTIA	25
HEADQUARTERS USAF		TDBTL	5
		TDBDP	5
AFCIN-3D2	1	AEDC (AEY)	1
ARL (ARB)	1	SSD (SSF)	2
		BSD (BSF)	1
OTHER AGENCIES		AFFTC (FTY)	1
		AFSWC (SWF)	1
CIA	1		
NSA	6		
DIA	9		
AID	2		
OTS	2		
AEC	2		
PWS	1		
NASA	1		
ARMY	3		
NAVY	3		
RAND	1		
PGE	12		
NAFEC	1		